

# **STABILITY ANALYSIS OF HIMALAYAN SLOPES**

MAJOR PROJECT II REPORT

SUBMITTED IN PARTIAL FULFILMENTS OF THE REQUIREMENTS

FOR THE AWARD OF THE DEGREE

OF

MASTERS OF TECHNOLOGY

IN

GEOTECHNICAL ENGINEERING

Submitted by:

**Faakirah Rashid**

**2K19/GTE/06**

Under the supervision of

**PROF. A.K.SAHU**



**DEPARTMENT OF CIVIL ENGINEERING**

DELHI TECHNOLOGICAL UNIVERSITY

(Formerly Delhi College of Engineering)

Bawana Road, Delhi-110042

AUG, 2021

# **DELHI TECHNOLOGICAL UNIVERSITY**

(Formerly Delhi College of Engineering)

Bawana Road, Delhi-110042

## **CANDIDATE'S DECLARATION**

I Faakirah Rashid, 2K19/GTE/06, student of M-tech, Geotechnical Engineering, hereby declare that this written submission represents my ideas in my own words and where other's ideas or words have been included. I have adequately cited and referenced the original sources. I also declare that I have adhered to all principles of academic honesty and integrity and have not misinterpreted or fabricated or falsified any idea/data/fact/source in my submission. I understand that any violation of the above will be cause for disciplinary action by the Institute and can also evoke penal action from the sources which have thus not been properly cited or from whom proper permission has not been taken when needed

Place: Delhi

(Faakirah Rashid Mir)

Date: 17/08/2021

**DEPARTMENT OF CIVIL ENGINEERING**

**DELHI TECHNOLOGICAL UNIVERSITY**

(Formerly Delhi College of Engineering)

Bawana Road, Delhi-110042

**CERTIFICATE**

I hereby certify that the Project dissertation work entitled “**Stability Analysis of Himalayan Slopes**” is a bonafide record of the work carried out by **Ms. Faakirah Rashid Mir (2K19/GTE/06)**, Department of Civil Engineering, Delhi Technological University, Delhi under my supervision and guidance, as a partial fulfillment for the award Of Masters Degree in Technology in the branch of Geotechnical Engineering. To the best of my knowledge this work has not been submitted in part or full for any Degree or Diploma to this University or elsewhere.

Place: Delhi

Date: 17/08/2021

**ANIL KUMAR SAHU**

**(PROFESSOR AND SUPERVISOR)**

## ABSTRACT

There is a large number of destabilized slopes in the Himalayan region mainly due to geological environment which is complex and having active tectonics present in the area. There is also deformation and metamorphism in the varied lithology of area which results in a rugged topography. The instability in the slopes is also being accelerated by the activities resulting from various ongoing construction and tunneling processes for the development in the region. There has been huge economic losses and a serious number of mishaps, which is endangering the Himalayan ecosystem due to various landslide related problems. The Himalayan region experiences frequent landslides along the national highways and mountain roads particularly the sections where there is debris slope. Factor of safety for each of the slopes under construction has been determined using numerical analysis first and then GEOSTUDIO correspondingly. In order to increase the stability of slope in the most efficient stabilization and ground improvement techniques have been proposed. It is very important that in the various vulnerable sections of the Himalayas slope stability assessment should be carried out. The site under consideration is Razdan Pass which is a high mountain pass at 3557m above the sea level. It is located in the Gurez valley of Jammu and Kashmir which is the highest point which connects Bandipora with Gurez. The road over the pass is winding and is called Bandipora-Gurez Highway. With NHPC Kishanganga Hydro Power Project Bandipore Jammu & Kashmir being in the vicinity and a new tunnel Razdan Pass Tunnel in the construction phase it becomes very important that stability of this slope is being assessed, for in many places over hundreds of meters the road is unprotected by the guardrails. Numerous tunnels have been constructed between 2007 and 2018 and also 37m tall concrete-face rock fill dam has been constructed during the construction of Kishanganga Hydro Power Project which adds to the already unstable slope which is snow covered for almost 6 months a year. Stability analysis of slopes using numerical analysis GEOSTUDIO is aimed at knowing about the factors that can potentially trigger a slope movement, understanding why a slope failure has occurred and, as well as the prevention of starting of such movement, at least slow it down or arrest it completely through mitigation countermeasures.

## **ACKNOWLEDGEMENT**

By the grace of almighty, I have great pleasure to place on record my deep and profound sense of gratitude and indebtedness to Prof. Yogesh Singh, Vice Chancellor, DTU, Prof V.K Minocha, Head of Department of Civil Engineer, my supervisor **Prof. Anil Kumar Sahu** for his inspiring guidance, constant encouragement, immense help and untiring enthusiasm, and above all, care and the interest he took throughout the course of this research work. His invaluable and unforgettable suggestions, in depth knowledge and affection, and patience always carried a personal touch and were constant source of inspiration for me. I am very much obliged to him for all this, which helped me to complete the study successfully and submit the thesis in the present form.

I further wish to place on record of our heartfelt gratitude and thanks to **Dr. Raju Sarkar**, coordinator Geotechnical Engineering and to all the faculties and support staff of the department of civil engineering.

Finally, I thank Delhi Technological University for providing all the facilities for successful completion of this study.

Date : 17/08/2021

(Faakirah Rashid Mir)

2K19/GTE/06

## CONTENTS

TITLE PAGE	
CANDIDATES DECLARATION.....	ii
CERTIFICATE.....	iii
ABSTRACT.....	iv
ACKNOWLEDGEMENTS.....	v
TABLE OF CONTENTS.....	vi
LIST OF TABLES.....	viii
LIST OF PLOTS.....	x
LIST OF FIGURES.....	xi
LIST OF ABBREVIATIONS.....	xii
CHAPTER 1: INTRODUCTION.....	1
1.1 General.....	1
1.2 Methodology for slope stability analysis.....	3
1.3 Need for the Project.....	4
1.4 Objectives.....	5
1.5 Working Plan.....	5
1.6 Site under consideration.....	6
CHAPTER 2: LITERATURE REVIEW.....	8
2.1 General.....	7
2.2 Literature review.....	7
2.3 Research Gap.....	11
CHAPTER 3: METHODS AND MATERIAL .....	12

3.1 Borehole data.....	12
3.2 Uniaxial compressive strength.....	15
3.3 Brazilian Tensile Strength.....	16
3.4 Modulus of Elasticity.....	17
3.5 Poisson’s Ratio.....	18
3.6 Numerical Analysis using Hoek Brown model.....	19
CHAPTER 4: RESULTS AND DISCUSSIONS.....	25
4.1 General Hoek Brown method.....	25
4.2 Calculations for Factor of Safety.....	28
4.3Dynamic Stability analysis.....	30
4.4 Performance based Earthquake Engineering(PBEE).....	31
4.5Software analysis using Geostudio.....	44
4.6 Results from software analysis.....	50
CHAPTER 5: CONCLUSIONS AND RECOMMENDATIONS FOR FUTURE WORK...	64
REFERENCES.....	65

## LIST OF TABLES

<b>S.No</b>	<b>TITLE</b>	<b>PAGE NO</b>
3.1	Test results for core recovery and RQD.	13
3.2	Various tests performed on rocks at site.	15
3.3	Uniaxial compressive strength of rocks in dry state.	15
3.4	Uniaxial compressive strength of rocks in saturated state.	16
3.5	Tensile strength of rocks at site	17
3.6	Effect of foliation/ schistosity direction on tensile strength (MPa)	17
3.7	Results of modulus of Elasticity in GPa	18
3.8	Results of Poisson's ratio.	18
3.9	Listing of mineralogy vis-a-vis hard and soft mineral assemblage	19
4.1	Hoek brown criterion values	26
4.2	Mohr Coulomb criterion values	26
4.3	Combined Hoek brown and Mohr Coulomb criterion values	28
4.4	Results of FOS values.	29
4.5	Peak ground acceleration calculations for different faults.	33
4.6	Unit weights for different rocks at site.	34
4.7	Shear wave velocity calculations.	34
4.8	Seismic coefficient calculations for D=5cm, $T_s = 0.378$	35
4.9	Seismic coefficient calculations for D=15cm, $T_s = 0.378$	35
4.10	Seismic coefficient calculations for D=30cm, $T_s = 0.378$	35
4.11	Seismic coefficient calculations for D=5cm, $T_s = 0.472$	38
4.12	Seismic coefficient calculations for D=30cm, $T_s = 0.472$	38
4.13	Seismic coefficient calculations for D=30cm, $T_s = 0.472$	38



4.14	Seismic coefficient dependence on fundamental period of sliding mass (D=5cm)	41
4.15	Seismic coefficient dependence on fundamental period of sliding mass (D=15cm)	41
4.16	Seismic coefficient dependence on fundamental period of sliding mass (D=30cm)	42
4.17	Lithological and structural description of rocks at site.	45

## LIST OF GRAPHS

SNO	TITLE	PAGE NO
4.1	Major principal stress vs minor principal stress in Hoek Brown model.	27
4.2	Major principal stress vs minor principal stress in Mohr Coulomb model.	27
4.3	Major principal stress vs minor principal stress in combined in both models.	28
4.4	Variation of seismic coefficient with peak ground acceleration (D=5cm), Ts=0.372	36
4.5	Variation of seismic coefficient with peak ground acceleration (D=15cm), Ts=0.372	36
4.6	Variation of seismic coefficient with peak ground acceleration (D=30cm), Ts=0.372	37
4.7	Combined variation of seismic coefficient with peak ground acceleration, ts=0.372	37
4.8	Variation of seismic coefficient with peak ground acceleration (D=5cm), Ts=0.472	39
4.9	Variation of seismic coefficient with peak ground acceleration (D=15cm), Ts=0.472	39
4.10	Variation of seismic coefficient with peak ground acceleration (D=30cm), Ts=0.472	40
4.11	Combined variation of seismic coefficient with peak ground acceleration ,Ts=0.472	40
4.12	Variation of seismic coefficient with fundamental period (D=5cm)	42
4.13	Variation of seismic coefficient with fundamental period (D=15cm)	43
4.14	Variation of seismic coefficient with fundamental period (D=30cm)	43
4.15	Combined variation of seismic coefficient with fundamental period (D=5cm)	44

## LIST OF FIGURES

FIG NO	DESCRIPTION	PAGE NO
1.1	Types of slope and causes of instability.	2
1.2	Landslide susceptibility map of India(2006)	4
3.1	GSI values depending upon rock structures and surface conditions.	22
4.4	Rock profile below the slope for a depth of 250m.	45
4.5	Input of the equivalent properties of $c$ , $\gamma$ and $\phi$ .	47
4.6	Geometrical construction of the slope at site.	47
4.7	Drawing of various regions.	48
4.8	Assigning the slip surface to the slope.	48
4.9	Calculation stage.	50
4.10	F.O.S calculation and slip surface generation for 50m depth and 100m length.	50
4.11	Body diagram for the forces acting on the slope.	51
4.12	F.O.S vs Lambda.	51
4.13	Variation of cohesion along the distance( horizontal).	52
4.14	Variation of Total normal stress along the distance ( horizontal).	52
4.15	Variation of shear resistance along the distance( horizontal).	53
4.16	F.O.S calculation and slip surface generation for 100m depth and 200m length.	53
4.17	F.O.S calculation and slip surface generation for 50m depth and 100m length showing all the slip surfaces.	54
4.18	F.O.S calculation and slip surface generation for 50m depth and	54
4.19	Body diagram for the forces acting on the slope.	55
4.20	F.O.S vs Lambda.	55
4.21	Variation of cohesion along the distance( horizontal).	56
4.22	Variation of Total normal stress along the distance ( horizontal).	56
4.23	Variation of shear resistance along the distance( horizontal).	57
4.24	F.O.S calculation and slip surface generation for 250m depth and 500m length	57
4.25	Body diagram for the forces acting on the slope.	58
4.26	F.O.S vs Lambda.	58
4.27	Variation of Total normal stress along the distance ( horizontal).	59
4.28	Variation of cohesion along the distance( horizontal).	59
4.29	Variation of shear resistance along the distance( horizontal).	60
4.30	F.O.S calculation and slip surface generation for 50m depth and 150m length.	60
4.31	F.O.S calculation and slip surface generation for 100m depth and 300m length.	61
4.32	F.O.S calculation and slip surface generation for 100m depth and 300m length.	61
4.33	F.O.S calculation and slip surface generation for 250m depth and 750m length.	62

## LIST OF SYMBOLS, ABBREVIATIONS AND NOMENCLATURE

<b>S.NO</b>	<b>SYMBOL</b>	<b>DESCRIPTION.</b>
1	$c'$	Effective unit cohesion
2	$d$	Effective normal stress
3	$\sigma$	Total normal stress
4	$u$	Pore water pressure
5	$\phi'$	Effective angle of internal friction
6	$s$	Shear Strength.
7	$mb$	Reduced material constant
8	$D$	Disturbance factor.
9	GSI	Geological strength index.
10	$Da$	Allowable displacement.
11	F.O.S	Factor of Safety.
12	$k$	Seismic Coefficient.
13	$\sigma_{ci}$	Uniaxaial compressive strength of intact rocks.
14	$\nu$	Poisson's ratio.
15	$S_a$	Peak Ground acceleration.



# CHAPTER 1

## INTRODUCTION

### 1.1 GENERAL

Slopes can occur in nature mainly in two forms:

1. Natural slopes.
2. Man made slopes.

Natural slopes are those which are formed by natural causes and are present in hilly areas Fig 1(a). The slopes formed by unnatural process are artificial slopes and are formed by humans as per requirements for example embankment slopes constructed for roads, railways, canals etc Fig 1(b). The slopes can be further classified in two groups (whether natural or man-made) as follows:

1. Infinite slope.
2. Finite slope.

The type of slope which is not having well defined boundaries and which is extending infinitely is called infinite slope Fig 1(a). The slope which is of limited extent is known as a finite slope. The engineers mostly deal with this type of slopes Fig 1.1(b)

#### **Slope Stability:**

“In the most simple ways by using limit equilibrium method “Stability of slopes “is determined by equating the shear strength and shear stresses of a slope at equilibrium. If forces that are driving the movement are lower than those resisting the movement, then the slope is considered to be stable. Factor of safety that is greater than 1.00 implies that the slope is stable. Factor of safety (F.O.S) is calculated by dividing the resistive forces by the driving forces.” (Hoek, 2002)

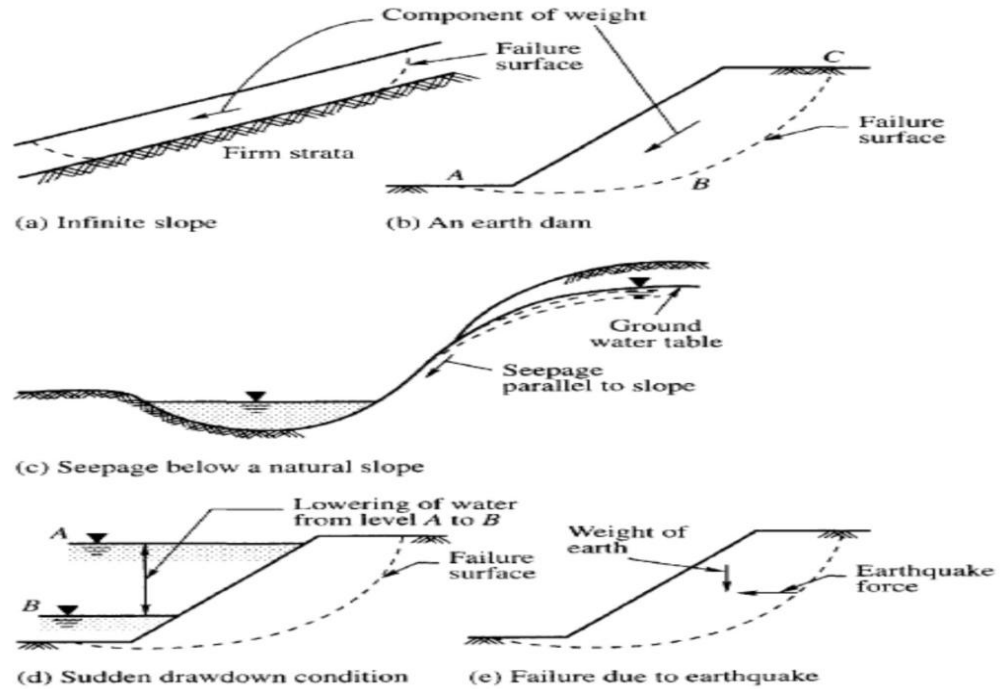


**Fig1.1. Types of slopes (a, b) and Causes of slope instability.**

**Assumptions used for the stability analysis of slopes:**

- The problem is assumed to be two dimensional.
- The shear strength of soil is assumed to follow Coulomb's law.
- $s = c' + d \tan \phi'$

where,  $c'$  - effective unit cohesion

$d =$  effective normal stress on the surface of rupture  $= (\sigma - u)$

$\sigma =$  total normal stress on the surface of rupture

$u =$  pore water pressure on the surface of rupture

$\phi' =$  effective angle of internal friction.

**Factor of safety**

The factor of safety with respect to shearing strength,  $F_s$ , may be written as

$$F_s = \frac{S}{\tau} = \frac{c' + \sigma' \tan \phi'}{\tau}$$

The shearing strength that is stabilized at each point of failure is written as

$$\tau = \frac{C'}{F_S} + \sigma' \frac{\tan \phi'}{F_S}$$

where  $\tau$ = shearing stress and  $S$  = shear strength of the material.

## 1.2 METHODOLOGY USED FOR SLOPE STABILITY ANALYSIS:

Before the start of use the analysis of slope by GEOSTUDIO it is preferable to fully grasp the knowledge of methodology of stability analysis and the numerical methods involved in this analysis. Slope stability analysis involves determination of the shear stresses that are developed along the rupture surface which is most likely to fail and the comparing the shear strength of the soil. The use of different models for different soil conditions are as follows:

### MOHR COULOMB MODEL:

Most of the geotechnical software uses Mohr Coulomb failure criterion so it becomes necessary to determine the cohesive strength and angle of internal friction for each rock mass and stress range. The curve is obtained by fitting an average linear relationship and it is a straight line. It is superimposed on the curve obtained from the Hoek Brown model. The results are given in the form of equations which involve an angle, cohesion in MPa and a linear relationship between major and minor principal stresses.

### HOEK BROWN CRITERION:

The failure criterion that was introduced by Hoek Brown provides a way for inputting the data for the analysis required for the design of the underground excavation in hard rock. The criterion provides a graph between the major and the minor principal stresses after considering the



uniaxial compressive strength, intact model parameter, Elastic modulus, GSI, model parameter and disturbance factor. It also takes into consideration the properties of the intact rock and then introduces the factors to reduce these parameters.

### 1.3 NEED FOR THE PROJECT

**Himalayan slopes have been chosen as the study area for Stability analysis:**

In India various types of landslides occur and especially in the Himalayas, particularly in monsoon season, including block falling, debris flow, debris slide, rock fall, rotational slip and crash. Area susceptible to landslide accounts for about a total 15% or 0.49 million km<sup>2</sup> of the terrain. According to the landslide Hazard zonation Map of India Fig (1.2) the most effected parts in India due to landslides are northern and western Himalayas.

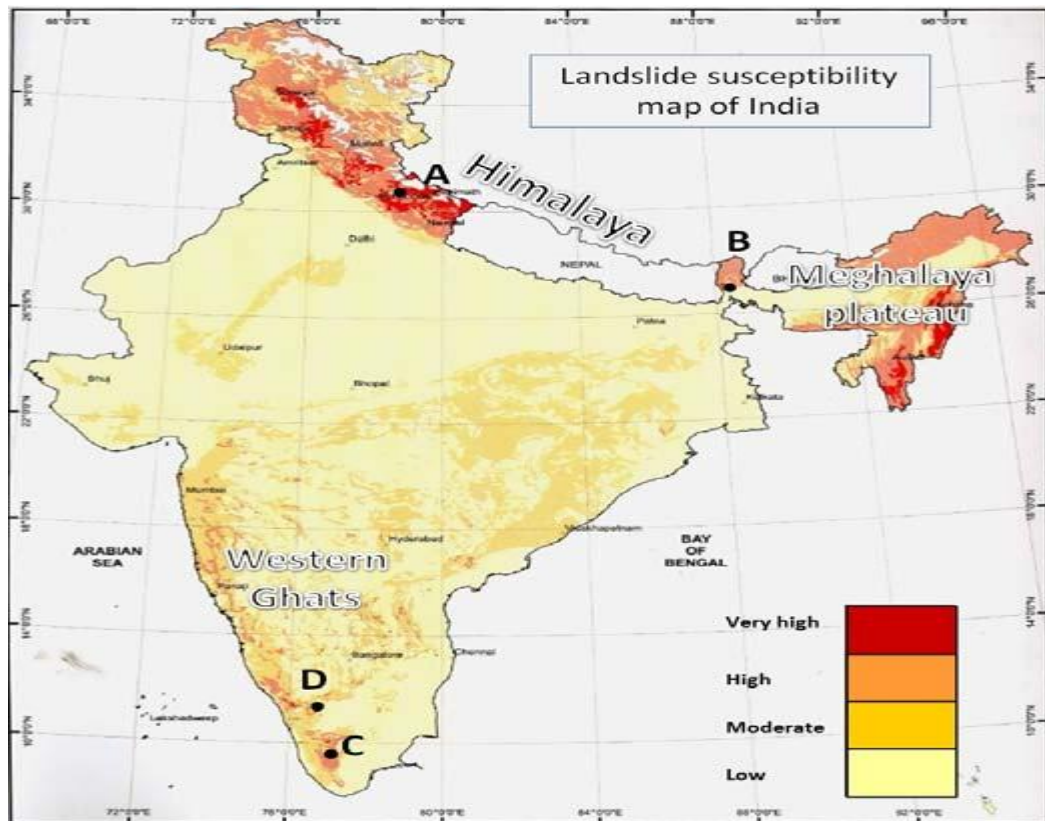


Fig 1.2. Landslide susceptibility map of India (2006). (Westen, 2012)

## **1.4 OBJECTIVES:**

- The main objective of the study was the calculation of Factor of safety of the slope which can then be used for designing the slope with optimal conditions with safety, reliability and economics.
- Locating the endangered areas and potential failure mechanisms which are obtained from the software analysis by GEOSTUDIO.
- Successful design of the slope requires site characteristics and geological information example height of slope, angle of the slope, groundwater conditions, properties of soil/rock mass, joint or discontinuity systems alternation of materials by faulting , movements and tension in joints, earthquake activity etc. These geological studies were made by studying the bore hole data and various reports of the site.
- The development and formation of natural slopes and the processes responsible for different natural features is understood while performing the analysis. Under both short-term and long term scenarios stability of slopes is assessed
- Effect of seismicity has been taken onto consideration and dynamic analysis of the slope has been carried out using Pseudo static slope stability analysis.

## **1.5 WORK PLAN:**

[1] Stability analysis is carried out firstly by using numerical methods. The methods that have been used for the numerical analysis are HOEK BROWN and MOHR COULOMB methods.

[2] Then in order to take into consideration the seismicity of the area Dynamic analysis has been carried out for which Pseudo static slope stability method has been used.

[3] Finally the analysis both static as well as dynamic has been carried out using GEOSTUDIO,

## **1.6 SITE UNDER CONSIDERATION:**

The site under consideration is Razdan Pass which is a high mountain pass at 3557m above the sea level. It is located in the Gurez valley of Jammu and Kashmir, It is the highest point which connects Bandipora with Gurez. The road over the pass is winding and is called Bandipora-Gurez Highway. With NHPC Kishanganga Hydro Power Project Bandipore Jammu & Kashmir being in the vicinity and a new tunnel Razdan Pass Tunnel in the construction phase it becomes very important that stability of this slope is being assessed, for in many places over hundreds of meters the road is unprotected by the guardrails. Numerous tunnels have been constructed between 2007 and 2018 including a 37 m tall concrete-face rock-fill dam through a 24 km (15 mi) tunnel during the construction of Kishanganga Hydro Power Project which adds to the already unstable slope which is snow covered for almost 6 months a year.

The slope is natural and infinite. It is having a height of 3300m and the data for analysis like uniaxial compressive strength, modulus of elasticity, GSI, Disturbance factor and all the lithological description of site has been taken from the data which was used while construction of HRT of NHPC Kishanganga project which is located across Razdan.

## CHAPTER 2

### LITERATURE REVIEW

#### 2.1 GENERAL

Stability analysis at a site provides the Factor of safety of the slope, whether it is safe or not. The analysis can be carried out both considering static (force and moment) and dynamic factors (pseudo static analysis). Using software for the process provides the slip surface, plots and factor of safety by providing the input parameters.

#### 2.2 LITERATURE REVIEW

Different authors have studied slope stability at various sites using different methods and a lot of software depending on the conditions at site. Dynamic slope stability provides a reduced Factor of safety taking into consideration the faults in the area and the geology of the area. The Probabilistic rock slope stability analysis for Himalayan conditions has been analyzed in a study (Shubh pathak and Bjorn Nilsen, 2004). The main focus of the study was the quantification of variable input parameters like groundwater pressure, active friction angle and seismic acceleration. This paper suggests that the stability analysis in the Himalayan region is very difficult for the conditions there are complex. Desandar back slope Kali gandaki hydropower project of Nepal is considered as a study area in this case.

Gali madhavi latha (2010) conducted studies for studying the rock slope stability using FLAC. The main purpose of the study was to understand the seismic stability of Himalayan rock slope. Railway bridge at about 350m above the ground level was considered, there is a crossing river and it connects the two blocks in Himalayas. The rock slope has very highly jointed rocks. Stability is studied numerically using program FLAC.

Rk umrao(2011) used Kinetic analysis in order to study the stability analysis of cut slopes mass rating in Rudraprayag district Utrakhand .The study was done for the mountain terrain of the Himalayas , i suggests that roads and highways play important role in stability of Himalayan slopes. The road considered is NH-109 which goes to the holy shrine of kedarnath and is thus very important.

TN Singh and AK VERMA (2012) studied the numerical simulation of landslide prone Himalayan region.As Himalayas are having geodynamic nature so the stability analysis is very difficult. Lower shivaliks have been taken as the study area. Laboratory experiments are also conducted to calculate the physiomechanical properties of the rock mass.

Hoek Brown (2002) provided a method that can be used for getting a relationship between the minor and the major principal stresses that are produced in the rock system by providing input parameters like GSI, uniaxial compressive strength of rocks, material constant, equivalent cohesion and angle of internal friction.

A.M Ahbab and M.J.S Safari (2020) studied the stability analysis by using a three-dimensional (3D) of the dam access road. F.O.S was acquired using a finite element code. The study revealed that by the increase in the level of water level F.O.S decreased and the soils entered in dam's reservoir. Slope excavation and water levels greatly influence the slope stability.

Jonathan D. Bray and Thaleia Travararou (2011) provided a method for calculating the seismic coefficient at a site which is representing the effects of earthquakes. This is based upon the seismic hazard curve and the amount of displacement that is taking place which can be considered safe for the design purposes.

Sarkar, S and Pain, A and Samanta, M (2015) studied the slopes that are vulnerable to failure in Sikkim Himalayas. These slopes were studied extensively as they cause a lot of damage to the nearby infrastructure when they fail. Deterministic approach was

used for the for obtaining the input parameters such as shear strength using the Generalized Hoek Brown method.

Weidong Wu et al (2019) studied the two dimensional dynamic analysis of seismic slope stability. The slip surface is obtained after the pseudo static analysis. Several failure criteria have been proposed to determine the stability of the slope. It is concluded that discrete element method along with the strength reduction technique is very feasible method for calculating the stability of the slope.

N.W.Xu and C.Sha and C.A Tang (2013) have demonstrated the micro seismic monitoring along the bank of a hydropower station (Jinping). The basic purpose of the study is that the slope of the dam should remain safe during the continuous excavation of the slope. Real time event location technique has been used for evaluating the evolution and migration of the seismic activity. Also some predictions has been made for the rock slope instability like the regions that were having damaged rocks have been identified.

Amanuel Zewdu (2020) was studying the modeling of embankment dam during stability analysis both static and dynamic. This dam in Ethiopia (Koga dam), it is an earth fill dam and the finite element based analysis has been done by PLAXIS 2D. The Mohr Coulomb criterion was used for the study purpose. The factor of safety at the end of construction for both static and dynamic were obtained.

Ashok K chugh (2003) conducted studies for the effect of the boundary conditions in the slope stability analysis. It was observed that these are having effects on the calculated factor of safety. In the limit equilibrium method there are certain boundary conditions which are common and have been illustrated in the form of a sample problem. Both 2D and 3D analysis has been carried out.

D.V. Griffiths (2004) emphasizes on the probabilistic slope stability analysis by finite element method. In this paper probabilistic tools have been used for the failure

analysis of a cohesive slope. Classical slope stability analysis has been used which treats shear strength as a random variable.

Maria Lia Napoli (2018) presented a stochastic approach to the slope stability in Bimrook. Both finite element and limit equilibrium method have been used. A lot of stability analysis were performed ( more than 90). This method has been introduced to take into account the spatial and dimensional variability of rock inclusions. The analysis has been carried out in MATLAB.

Xiao- Li Yang and Jian – Hua Yin (2004) were studying the stability analysis of slopes having non linear failures as mostly geo-materials are having a non linear strength envelope. Mohr coulomb failure criterion has been used and the non linear criterion has been approximated with a generalized technique.

Tamotsu Matsui (1992) studied the strength reduction techniques for being used in the slope stability analysis by finite element methods. The slope failure in this study has been defined by the shear strength criterion. The safety factor is related to the average of local factor of safety along the failure slip surface. How this method can be used for practical design that has also been demonstrated.

Zheng Yingren (2010) explains the limitations of evaluating the dynamic stability using the Pseudo static slope stability methods. The software that has been used for analysis is FLAC, which takes into consideration the fracture plane of slope being analyzed and failure mechanisms. This paper also represents the dynamic history of the area which is dependent on the tensile-shear failure. The dynamic analysis uses strength reduction and shear failure. The paper includes a complete dynamic method for stability analysis.

Wanying He and Defa Guo (2015) used double safety factors and dynamic local shear strength reduction for analysis of dam slope stability. The study takes a different approach and uses different reduction factors associated with material strength factors

like slope cohesion and internal angle of friction. They have used yield approach index (YAI) criterion. The factor of safety that has been obtained is less than the traditional approach.

### **2.3 RESEARCH GAP:**

There are a lot of papers on slope stability analysis but much work hasn't been done on the Dynamic analysis of the slopes. Papers are available where seismic monitoring has been done but these are international papers, such studies where geology of the area is considered, effect of faults and seismicity is considered are less. Ground water table play and important role in stability analysis and it has not been studied to that extent.



## CHAPTER 3

### MATERIALS AND METHODS

#### 3.1 BOREHOLE DATA:

In geotechnical site investigation boreholes are widely used as they have minimal environmental impact and they are cost effective method of sampling materials. The graphic core logs provide a record of both the natural features intersected by drilling, and the instrumentation and testing locations in each borehole

All of the bore hole data has been tabulated using excel sheets and the following observations have been made from this data:

##### (a) Borehole data for Dam site:

- Depth of boring is 40m, type of core barrel is double tube, type of bit is diamond, drilling agency is Space engineers consortium (P) ltd. Collar elevation is 2366.14m and ground elevation is 2366.13m. co ordinates of the site are E 27840.29 and N 27342.82.
- Angle with horizontal is 90°
- Data obtained from the bore-hole log is as follows: Lithological description after every 1m of core advance.
- Sizes of core pieces ( <10mm, < 10-25mm,<25-75mm,<150mm).
- Percentage core recovery.
- Percentage Rock Quality Designation (RQD).
- Structural description..
- Deth of water table in meters.
- Standard penetration test values.

##### Percentage Core recovery:

The amount of the rock that is drilled out or withdrawn as core in rock core drilling, it is generally expressed as a percentage. The values of core recovery have been tabulated in table number (1.2).

### Rock quality designation Percentage:

Rock quality designation (RQD) gives an estimate of rock strength at the site. RQD of more than 75% means that the rock is high quality, low quality of less than 50%. The values of RQD for after every 1 meter in the bore hole have been tabulated in the following table.

**Table 3.1: Test results for core recovery and RQD.**

Depth in m	Percentage core recovery	Percentage RQD
0.5-1	-	-
1.5-2	-	-
2.5-3	4	-
3.5-4	33	10
4.5-5	23	-
5.5-6	50	25
6.5-7	35	-
7.5-8	22	-
8.5-9	31	-
9.5-10	40	-
10.5-11	50	24
11.5-12	51	20
12.5-13	48	22
13.5-14	64	35
14.5-15	56	13
15.5-16	45	15
16.5-17	36	-
17.5-18	26	-
18.5-19	34	-
19.5-20	33	-
20.5-21	36	-
21.5-22	60	-
22.5-23	75	71
23.5-24	85	85
24.5-25	83	76
25.5-26	92	75
26.5-27	95	27
27.5-28	96	48
28.5-29	87	4
29.5-30	83	12
30.5-31	89	73
31.5-32	97	54
32.5-33	99	98

33.5-34	93	76
34.5-35	98	94
35.5-36	99	90
36.5-38	99.5	98
38.5-40	99.5	99.5

(b) Bore-hole data for HRT site:

A similar bore hole data log has been prepared at HRT Site which provides similar properties as mentioned in the dam site log.

- Depth of boring is 250m, type of core barrel is double tube, type of bit is diamond, drilling agency is Arihant Drillings. Collar elevation is 3428.84 m and ground elevation is 3428.83 m. co ordinates of the site are E 17419.17 and N 13378.96.
- Angle with horizontal is 90°
- Data obtained from the bore-hole log is as follows: Lithological description after every 1m of core advance till 250m and structural description of rocks after every 1m which helps in evaluating the geological strength index of the site.

**Since the borehole data that has been used for HRT site is every extensive (250 entries) it has not been included here and is attached with the reports.**

After studying the bore hole data at the site it was observed that the rocks which were abundant at site were as follows:

- Phyllitic Quartzite.
- Quartzitic Phyllite.
- Granodiorite.
- Silstone

Various rock mechanics tests were performed on these rocks for determining their engineering properties. The type of tests performed and the engineering properties determined have been given in the following table:

**Table 3.2: Various tests performed on rocks at site.**

Type of test performed	Engineering property obtained
Uniaxial compressive strength ( Dry)	Compressive strength.
Uniaxial compressive strength ( Saturated)	Compressive strength.
Brazilian tensile test.	Tensile strength.
MTS stiff testing test sing strain gauges	Modulus of Elasticity.
MTS stiff testing test sing strain gauges	Poison's Ratio.
Passing test	Brittleness index.
Penetration test	Seivers J value .
Drilling test	Drilling rate index.
Bore hole data	Rock Quality designation(RQD%)

### 3.2 UNIAXIAL COMPRESSIVE STRENGTH:

Uniaxial compressive strength of rocks is one of the most important mechanical property that is used for the engineering design related problems. The UCS of rocks was calculated in both dry and saturated state using stiff testing machine under controlled loading rate. The results have been tabulated in table 3 and 4.

**Table 3.3: Uniaxial compressive strength of rocks in dry state.**

S.no	Uniaxial Compressive Strength in Mpa	S.no	Uniaxial Compressive Strength in Mpa	S.no	Uniaxial Compressive Strength in Mpa	S.no	Uniaxial Compressive Strength in Mpa
	Phyllitic Quartzite		Quartzitic Phyllite		Granodiorite		Siltstone
1	127.79	1	19.67	1	107.62	1	37.7
2	106.10	2	36.56	2	124.82	2	31.63
3	103.44	3	23.58	3	108.64	3	61.75
4	109.75	4	16.05	4	148.94	4	46.6
5	80.54	5	27.51	5	131.28	5	70.51
6	109.07			6	114.71		
Avg	106.12	Avg	24.67	Avg	122.67	Avg	49.64

The Dry UCS was lowest for Quartzitic Phyllite rock (24.67MPa) and the highest for Grano-diorite( 122.67MPa). The value of UCS for siltstone and Phyllitic Quartzite are in between. The Uniaxial Compressive strength of rock samples were also determined using stiff testing machine after immersing them in water for 72 hours. The results are tabulated as follows:

**Table 3.4:Uniaxial compressive strength of rocks in saturated state.**

S.no	Uniaxial Compressive Strength in MPa	S.no	Uniaxial Compressive Strength in MPa	S.no	Uniaxial Compressive Strength in MPa	S.no	Uniaxial Compressive Strength in MPa
	Phyllitic Quartzite		Quartzitic Phyllite		Granodiorite		Siltstone
1	111.79	1	12.11	1	124.19	1	28.87
2	96.01	2	25.51	2	125.66	2	37.13
3	79.02	3	7.22	3	116.98	3	51.74
				4	126.95		
				5	110.31		
				6	113.21		
Avg	95.61	Avg	14.95	Avg	119.55	Avg	39.25

The UCS (Saturated) was found to be lower than the corresponding strength in dry condition. This was the lowest for quartzitic phyllite rock ( 14.95 MPa) and highest for grano-diorite(119.55 MPa). Quartzitic phyllite, Granodiorite, Silstone have shown a marginal change in their strength after saturation. The absorption of water was not appreciable in these rocks. The reduction of strength was noticeable in Quartzitic phyllite due to marked increase in water absorption.

### **3.3 BRAZILIAN TENSILE STRENGTH:**

Tensile strength of rock samples was done by an indirect method and the results are presented in table 4. To study the influence of foliation direction with respect to the axis of loading a few more tests were conducted for two rock types namely quartzitic phyllite and silstone where such schstocity anisotropy is prominent. The results have revealed interesting facts. The variartion in tensile strength in perpendicular direction( with repect to loading axis was 1.5 times more than that of the strength in parallel

direction for quartzitic phyllite. However, for siltstone this ratio was 1.2 times. The details are shown in table 5.

**Table 3.5 : Tensile strength of rocks at site.**

Sample No	Tensile Strength in MPa	Sample No	Tensile Strength in MPa	Sample no	Tensile Strength in MPa	Sample no	Tensile Strength in Mpa
	Phyllitic Quartzite		Quartzitic Phyllite		Granodiorite		Siltstone
1	9.23	1	4.88	1	8.76	1	10.63
2	15.24	2	4.11	2	12.43	2	10.82
3	14.46	3	6.2	3	8.43	3	10.51
4	19.22	4	8.29	4	9.89	4	8.57
5	15.63			5	9	5	7.14
Average	14.76	Average	5.87	Average	9.7	Average	9.53

The Brazilian tensile strength was the highest for phyllitic quartzite(14.76MPa) and the lowest for Quartzitic Phyllite(5.87MPa) where as the values of granodiorite and siltstone are in between.

**Table 3.6:effect of foliation/ schistocity direction on tensile strength (MPa)**

Sno	Quartzitic Phyllite	Sno	Perpendicular	Sno	Siltstone	Sno	Perpendicular
	Parallel				Parallel		
1	4	1	6.31	1	11.8	1	11
2	4.21	2	6.45	2	9.1	2	10.2
		3	6.46	3	6.6	3	11.8
Avg	4.1	Avg	6.41	Avg	9.2	Avg	11
Sno	Parallel	Sno	Perpendicular	Sno	Parallel	Sno	Perpendicular

### 3.4 MODULUS OF ELASTICITY( GPa):

Rock properties, namely, modulus of elasticity and poisson's ration were determined under MTS stiff testing machine using strain gauges ( balanced) and the data was acquired by a data accusation system( SPYDER 8). The same was analysed and presented in table 6 and 7.

**Table 3.7: Results of modulus of Elasticity in GPa.**

Sample No	Elastic Modulus Gpa	Sample No	Elastic Modulus Gpa	Sample No	Elastic Modulus Gpa	Sample no	Elastic Modulus Gpa
	Phyllitic Quartzite		Quartzitic Phyllite		Granodiorite		Siltstone
1	79.6	1	8.3	1	66.4	1	50.5
2	74.1	2	23.6	2	63.3	2	36.5
3	69.9	3	3.3	3	60.3	3	46.5
4	68	4	24.5	4	69.1	4	50
5	61.9			5	55.2	5	26.8
Avg	70.7	Avg	14.9	Avg	62.9	Avg	42.1

The modulus of elasticity was the highest for Phyllitic quartzite 79.6GPa and the lowest for Quartzitic Phyllite (14.9 GPa) where as the values of Granodiorite and siltstone lie in between.

### 3.5 POISSON'S RATIO:

It is the ratio of the longitudinal strain to the lateral strain that is produced in the a body/ core sample when it is stressed during various processes.

**Table3.8: Results of Poisson's ratio.**

S.no	Poisson's Ratio	S.no	Poisson's Ratio	S.no	Poisson's ratio Granodiorite	S.no	Poisson's ratio Siltstone
	Phyllitic Quartzite		Quartzitic Phyllite				
1	0.28	1	0.11	1	0.13	1	0.18
2	0.18	2	0.33	2	0.17	2	0.1
3	0.17	3	0.14	3	0.1	3	0.19
4	0.16			4	0.24	4	0.21
5	0.14			5	0.14		
Avg	0.19	Avg	0.22	Avg	0.15	Avg	0.17

**Table3. 9: Listing of mineralogy vis-a-vishard and soft mineral assemblage.**

S.no	Rock type	Hard minerals	percentage	Soft minerals	percentage	Remarks
1	Phyllitic Quartzite	Quartz	35-40%	Mica	5-8%	Fine grained
		Feldspar	5%	Clay	20%	rock with finer
		Opauques	1-2%	Other accessory minerals (includes matrix)	25%	quartz veinlets
2	Quartzitic Phyllite	Quartz	30-33%	Mica	2%	Fine grained
		Iron oxide	3%	Clay	40-60%	Massive, coarse crystalline rock
		Feldspar	2%			
	Alkali	40%				
	Plagioclase					
	Granodiorite	Feldspar				
		Amphibole	25%			
Quartz		25%				
Pyroxine		10%				
4	Siltstone	Quartz	30%	Carbonates	60%	very fine grained with
				clay	10%	splution activity

### **3.6 NUMERICAL ANALYSIS OF SITE USING HOEK BROWN METHOD:**

The failure criterion that was introduced by Hoek brown provides a way for inputting the data for the analysis required for the design of the underground excavation in hard rock. The criterion provides a graph between the major and the minor principal stresses after considering the uniaxial compressive strength, intact model parameter, Elastic modulus, GSI, model parameter and disturbance factor. It also takes into consideration the properties of the intact rock and then introduces the factors to reduce these parameters.

Hoek-Brown criterion, is defined by the equation:



$$\sigma_1' = \sigma_3' \times \sigma_{ci} \left[ m_i \left( \frac{\sigma_3'}{\sigma_{ci}} \right) + s \right]^{0.5} \quad [3.1]$$

where  $\sigma_1'$  and  $\sigma_3'$  are the major and minor effective principal stresses at failure  
 $\sigma_{ci}$  is the uniaxial compressive strength of the intact rock material and

$m$  and  $s$  are material constants,

where  $s = 1$  for intact rock.

Hoek and Brown equations are used in combination with the Balmers equations which give a relation between major and minor principal stresses and normal and shear stresses. Then factor of safety is calculated using the strength parameters.

### 3.6 (a) GENERALIZED HOEK-BROWN CRITERION:

“This is expressed as

$$\sigma_1' = \sigma_3' \times \sigma_{ci} \left[ mb \left( \frac{\sigma_3'}{\sigma_{ci}} \right) + s \right]^a \quad [3.2]$$

where  $mb$  is a reduced value of the material constant  $m_i$  and is given by

$$m_b = m_i \exp \left[ \frac{GSI - 100}{28 - 14D} \right] \quad [3.3]$$

$s$  and  $a$  are constants for the rock mass given by the following relationships:

$$s = \exp \left[ \frac{GSI - 100}{9 - 3D} \right] \quad [3.4]$$

$$a = \frac{1}{2} + \frac{1}{6} \left[ \exp \frac{-GSI}{15} - \exp \frac{-20}{3} \right] \quad [3.5]$$

$D$  is a factor which is dependent on the rock mass disturbance that is being imparted to it by blast damage and stress relaxation. It is having values which varies from 0 for rocks which are undisturbed in situ rock masses to 1 for very disturbed rock masses.

The uniaxial compressive strength is obtained by

$$\sigma_c = \sigma_{ci} s^a \quad [3.6]$$

and, the tensile strength is:

$$\sigma_t = \frac{-s\sigma_{ci}}{mb} \quad [3.7] \text{'' (Hoek, 2002)}$$

[1] Modulus of deformation:







Young's modulus or Modulus of elasticity was obtained from using the MTS stiff testing machine along with the strain gauges (balanced). The modulus of elasticity obtained at the site needs to be reduced on account of GSI and disturbance factor. The rock mass stiffness  $E_{rm}$  can be estimated after considering the effect of GSI and D (disturbance factor) from the following empirical equation:

$$E_{rm} = E_i \left[ 0.02 + \frac{1-D/2}{1+e^{\frac{60+15D-GSI}{11}}} \right] \quad [3.8]$$

[2] Geological strength index (GSI):

“This GSI Index is based upon the based on the structure and condition of discontinuity surfaces in the rock mass , the lithology of the area, and it is evaluated from visual examination of the rock mass that is in the open while surface excavation is conducted in places such as borehole cores. The geological strength index is calculated by considering the combination of the two fundamental parameters of geological process the conditions of discontinuities and the blockiness of the mass.” (Hoek, 2002)

From the borehole data it was observed that the rock that was in abundance at the site is Siltstone. It exists almost uniformly throughout the depth of 250 m that has been considered for examination except for few meters where Phyllitic Quartzite occurs.. It is having lithological structure as foliated highly fractured rock and jointed at  $76^\circ$  with horizontal and Structural description as weathered iron stained fractured rock of siltstone having phyllitic characteristics. From this information the GSI of site was measured to be in the range of 40-50 and an average value of **45 GSI** has been used in the analysis.

<p><b>GEOLOGICAL STRENGTH INDEX FOR JOINTED ROCKS (Hoek and Marinos, 2000)</b></p> <p>From the lithology, structure and surface conditions of the discontinuities, estimate the average value of GSI. Do not try to be too precise. Quoting a range from 33 to 37 is more realistic than stating that GSI = 35. Note that the table does not apply to structurally controlled failures. Where weak planar structural planes are present in an unfavourable orientation with respect to the excavation face, these will dominate the rock mass behaviour. The shear strength of surfaces in rocks that are prone to deterioration as a result of changes in moisture content will be reduced is water is present. When working with rocks in the fair to very poor categories, a shift to the right may be made for wet conditions. Water pressure is dealt with by effective stress analysis.</p>		SURFACE CONDITIONS				
STRUCTURE		VERY GOOD	GOOD	FAIR	POOR	VERY POOR
		Very rough, fresh unweathered surfaces	Rough, slightly weathered, iron stained surfaces	Smooth, moderately weathered and altered surfaces	Slickensided, highly weathered surfaces with compact coatings or fillings or angular fragments	Slickensided, highly weathered surfaces with soft clay coatings or fillings
		DECREASING SURFACE QUALITY →				
	INTACT OR MASSIVE - intact rock specimens or massive in situ rock with few widely spaced discontinuities	90			N/A	N/A
	BLOCKY - well interlocked undisturbed rock mass consisting of cubical blocks formed by three intersecting discontinuity sets	80	70			
	VERY BLOCKY- interlocked, partially disturbed mass with multi-faceted angular blocks formed by 4 or more joint sets		60	50		
	BLOCKY/DISTURBED/SEAMY - folded with angular blocks formed by many intersecting discontinuity sets. Persistence of bedding planes or schistosity			40	30	
	DISINTEGRATED - poorly interlocked, heavily broken rock mass with mixture of angular and rounded rock pieces				20	
	LAMINATED/SHEARED - Lack of blockiness due to close spacing of weak schistosity or shear planes	N/A	N/A			10
	↓ DECREASING INTERLOCKING OF ROCK PIECES					

**Fig 3.3: GSI values depending upon rock structures (Hoek, 2002)**

3.6 (b) MOHR-COULOMB CRITERION:

Most of the geotechnical software uses Mohr Coulomb failure criterion so it becomes necessary to determine the cohesive strength and angle of internal friction for each rock

mass and stress range. The curve is obtained by fitting an average linear relationship by solving equation 2 and it is a straight line. It is superimposed on the curve obtained from the Hoek Brown model. The results are given in the form of equations which involve an angle, cohesion in MPa and a linear relationship between major and minor principal stresses.

“This gives results in the form of the cohesive strength and angle of friction:

$$\Phi' = \sin^{-1} \left[ \frac{6amb (s+mb\sigma_{3n}')^{a-1}}{2(1+a)(2+a)6amb (s+mb\sigma_{3n}')^{a-1}} \right] \quad [3.9]$$

$$c' = \frac{\sigma_{ci}[(1+2a)s+(1+a)mb\sigma_{3n}'] (s+mb\sigma_{3n}')^{a-1}}{(1+a)(2+a)\sqrt{1+6amb (s+mb\sigma_{3n}')^{a-1}}/(1+a)(2+a)} \quad [3.10]$$

$$\text{where } \sigma_{3n}' = \sigma_{3\text{max}}' / \sigma_{ci} \quad [3.11]$$

The equivalent plot defined by major and minor principal stresses is given by :

$$\sigma_1' = \frac{2c \cos \phi}{1 - \sin \phi} + \frac{1 + \sin \phi}{1 - \sin \phi} \sigma_3' \quad [3.12]$$

[1] Determination of  $\sigma'_{3\text{MAX}}$ :

The value of  $\sigma'_{3\text{MAX}}$  is given from an equivalent characteristic equation and curves:

$$\frac{\sigma'_{3\text{MAX}}}{\sigma_{cm}'} = 0.47 \left[ \frac{\sigma_{cm}'}{\sigma_o} \right]^{-0.94} \quad [3.13]$$

Where  $\sigma_o$  are the insitu stresses and  $\sigma_{cm}'$  is given by the equation:

$$\sigma_{cm}' = \sigma_{ci} \frac{(mb+4s-a(mb-8s)) \left( \frac{mb}{4} + s \right)^{a-1}}{2(1+a)(2+a)} \quad [3.14]$$

[2] Estimation of disturbance factor (D):

In the Hoek Brown Criterion, for undisturbed rocks insitu rock masses (D) is taken to be zero. When the effect of heavy blasting is taken into consideration it is considered that for the “disturbed rock mass” “D=1”. Since the tunnel boring was done partly by using Tunnel boring machine which is having a D=0 and partly by drill blasting method in strong rocks (D=0.5) an average **D=0.25** has been used in the analysis.

[3] Intact rock parameter(  $m_i$ ):

$m_i$  is called the intact rock parameter , it is an empirical parameter , values of which are given in a table proposed by Hoek Brown, 1980, Hansen, 1988 and Hoek et al 1998.” (Hoek, 2002)

## CHAPTER 4

### RESULTS AND DISCUSSION

#### 4.1 GENERALISED HOEK BROWN ANALYSIS:

From studying the data it was observed that Siltstones are abundance at the site and are having the lowest Uniaxial Compressive strength in saturated state as 39.25MPa and lowest Elastic modulus as 42.1 GPa so the data values of this rock have been used for the numerical analysis for having a more valid design having high FOS. The value of  $m_i$  for Siltstone from the table is 9.

$$GSI = 40-50$$

$$\text{Average value of GSI} = 45$$

$$D = 0.25$$

$$m_i = 9$$

$$m_b = 9 \exp \left[ \frac{45-100}{28-14(0.25)} \right]$$

$$m_b = 0.953$$

$$s = \exp \left[ \frac{45-100}{9-3*0.25} \right]$$

$$S = .0012$$

$$a = \frac{1}{2} + \frac{1}{6} \left[ \exp \frac{-45}{15} - \exp \frac{-20}{3} \right]$$

$$a = .508 = .5$$

$$\sigma_c = (39.25) (0.0012)^{0.508}$$

$$\sigma_c = 1.2884 \text{MPa}$$

$$\sigma_1' = \sigma_3' + 39.25 (.953 * (\sigma_3' / 39.25) + .0012)^{0.5}$$

This is the equation that is obtained after Hoek brown numerical analysis. From this equation a plot is made between the major and minor principal stresses.

$$\sigma_{cm}' = 39.25 \frac{(0.953 + 4 * 0.0012 - 0.5(.953 - 8 * 0.0012)) \left( \frac{0.953}{4} + 0.0012 \right)^{0.5-1}}{2(1+0.5)(2+0.5)}$$

$$\sigma_{cm} = 5.068 \text{MPa}$$

$$\frac{\sigma_3' \text{MAX}}{5.068} = 0.47 \left[ \frac{5.068}{1.2884} \right]^{-0.94}$$

$$\sigma_{3\text{max}} = 0.657 \text{MPa}$$

$$\sigma_{3n} = 0.657 / 39.25$$

$$\sigma_{3n} = 0.0167$$

$$\Phi' = \sin^{-1} \left[ \frac{60.5 \cdot 953 (0.0012 + 0.95 \cdot 0.0162)^{0.5-1}}{2(1+0.5)(2+0.5) \cdot 5 \cdot 953 (0.0012 + 953 \cdot 0.158)^{0.5-1}} \right]$$

$$\Phi' = 47.70^\circ$$

$$c' = \frac{14.95[(1+2 \cdot 5)0.0012 + (1+0.5)0.953 \cdot 0.0167](0.0012 + 953 \cdot 0.0167)^{0.5-1}}{(1+0.5)(2+0.5) \sqrt{1 + 60.5 \cdot 9530 (0.0012 + 0.953 \cdot 0.158)^{0.5-1}} / (1+5)(2+5)}$$

$$c' = 0.2969 \text{ Mpa} = 296.9 \text{ kpa}$$

$$\sigma_1' = \frac{2c \cos 48.58}{1 - \sin 48.58} + \frac{1 + \sin 48.58}{1 - \sin 48.58} (\cdot 1188)$$

$$\sigma_1 = 1.534 + 6.68 * \sigma_3$$

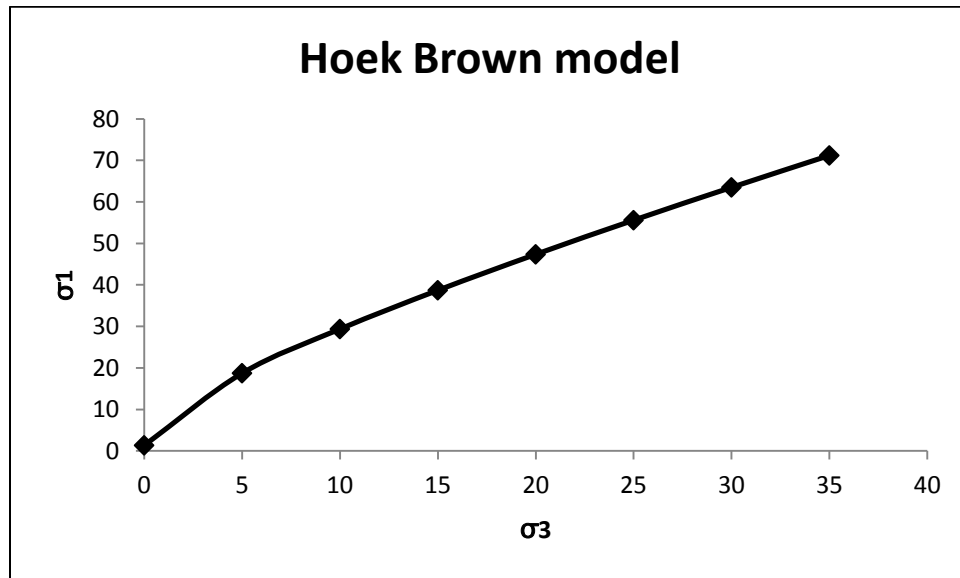
This is the equation that is obtained after Mohr Coulomb numerical analysis. From this equation a plot is made between the major and minor principal stresses.

**Table 4.1 :Hoek Brown criterion values**

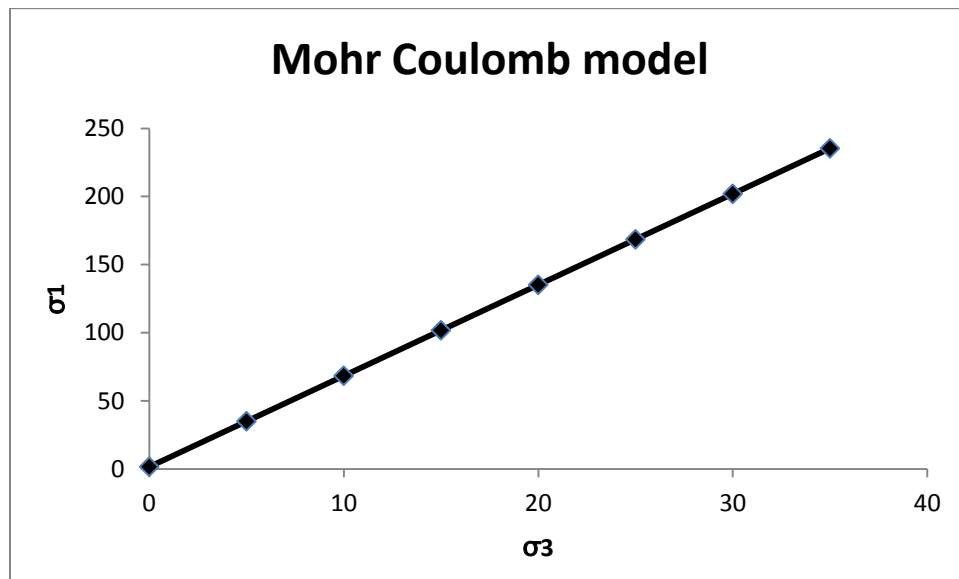
HOEK BROWN MODEL	
$\sigma_1$ (Mpa)	$\sigma_3$ (Mpa)
1.359	0
18.743	5
29.388	10
38.726	15
47.385	20
55.61	25
63.52	30
71.208	35

**Table 4.2: Mohr Coulomb criterion values**

MOHR COULOMB MODEL	
$\sigma_1'$ (Mpa)	$\sigma_3'$ (Mpa)
1.534	0
34.934	5
68.334	10
101.734	15
135.134	20
168.534	25
201.934	30
235.334	35



**Graph 4.1: Major principal stress vs minor principal stress in Hoek brown model.**

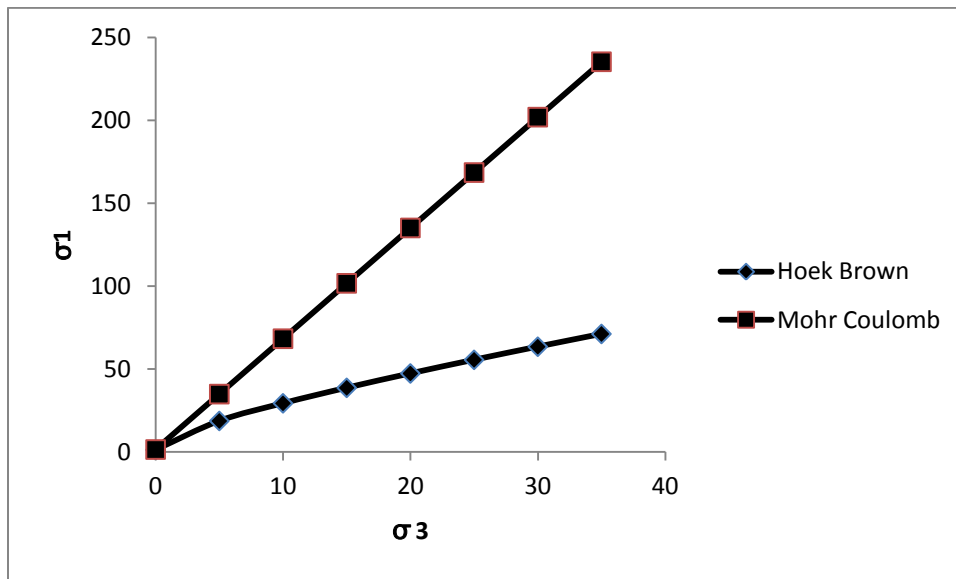


**Graph 4.2: Major principal stress vs minor principal stress in Mohr Coulomb model.**



**Table 4.3: Combined Hoek Brown and Mohr Coulomb criterion values**

$\sigma_3'$ (MPa)	$\sigma_1'$ (MPa)	$\sigma_1'$ (MPa)
0	0.5178	0.6284
5	13.456	35.6
10	21.92	70.588
15	29.62	105.47
20	36.88	140.42
25	43.87	175.37
30	50.68	210.32
35	57.33	245.27



**Graph4. 3: major principal stress vs minor principal stress in combined in both models.**

#### **4.2 CALCULATIONS FOR THE FACTOR OF SAFETY:**

Factor of safety after considering strength is given by :

$$FS = \frac{S}{\tau} = \frac{C' + \sigma_n' \tan \phi'}{\tau}$$

where S is the strength of the rock in which  $c=0.296$  Mpa and  $\Phi'=47.70^\circ$

$\sigma_n$  is the normal stress at the site and  $\tau$  is the shear stress in Mpa.

Principal major and minor stresses  $\sigma_1, \sigma_3'$  are related to the Normal and Shear stresses have been calculated by the equations proposed by Balmers.

$$\sigma_n' = \frac{\sigma_1' + \sigma_3'}{2} - \frac{\sigma_1' - \sigma_3'}{2} * \frac{x-1}{x+1}$$

$$\text{where } x = 1 + a m_b (m_b \sigma_3' / \sigma_{ci} + s)^{a-1}$$

$$z = x^{0.5} / x + 1$$

$$\text{where } \sigma_{ci} = 39.25 \text{ Mpa}$$

$$\tau = (\sigma_1' - \sigma_3) * z$$

$$s = c + \sigma_n \tan(\phi)$$

$$a = 0.508$$

$$s = 0.0012$$

$$m_b = 0.953$$

The value of  $\sigma_1, \sigma_3'$  have been taken from table 12 and the value of factor of safety have been calculated for various major and minor principal stress values.

**Table 4.4: value of factor of safety.**

X	(X-1)/ (X+1)	( $\sigma_1' + \sigma_3'$ )/2	( $\sigma_1' - \sigma_3'$ )/2	$\sigma_n'$	Z	$\sigma_1' - \sigma_3'$	S	T	F.O.S
14	0.86	0.679	0.679	.09	.249	1.35	.395	.338	1.16
2.35	0.40	11.87	6.871	9.09	.457	13.7	10.2	6.28	1.89
1.96	0.32	19.69	9.694	16.53	.472	19.3	18.4	9.15	2.15
1.79	0.28	26.86	11.863	23.49	.479	23.7	26.1	11.3	2.36
1.68	0.25	33.69	13.962	30.18	.483	27.3	33.4	13.2	2.54
1.61	0.23	40.30	15.305	36.69	.485	30.6	40.6	14.8	2.71
1.56	0.22	46.76	16.76	43.07	.487	33.5	47.6	16.3	2.86
1.52	0.20	53.10	18.104	49.35	.489	36.2	54.5	17.7	2.99

Factor of safety is in the range of 1.16 to 2.99 implying that the slope is stable.

#### 4.3 DYNAMIC SLOPE STABILITY ANALYSIS:

**“Bray and Travasarou method:** The method that has been adopted for carrying out the dynamic analysis of the site under consideration is **“Pseudo Static Slope Stability analysis.”**In Earthquake engineering this method is very uncomplicated and is used for the assessment of seismic response of the Slopes and embankments. There is use of the seismic coefficient in this procedure, it is applied to the potential sliding mass and it represents the damaging effect of earthquake shaking. The selection of seismic coefficient that is used in this analysis is based on seismic hazard and seismic displacement that are very important for the seismic stability of slope. The design procedure involves calculation of seismic coefficient that is directly a function of allowable seismic displacement and seismic hazard at project site.” (Bray, 2011)

The factor of safety is calculated by the method of static limit equilibrium where a horizontal earthquake induced inertial force (product of seismic coefficient (k) and weight (W) of the sliding mass) is applied to potential sliding mass. Also there is calculation of the dynamic strength (S) of the material.

$$F.O.S = \frac{\text{Resisting force}}{\text{Driving Force}} = \frac{kW}{S}$$

“The horizontal force kW represents dynamic consequence of the design earthquake. But this acts as a Pseudo static force as it applies only in one direction unlike the actual seismic wave which is in one direction in one second and in the opposite direction in the one tenth of the second. Newmark(1965) realized that these are transient pulses and the result of these forces will be a series of displacement pulses. The performance of the structure is determined by whether or not the permanent displacement that is induced by the seismic displacement is tolerable or not.” (Bray, 2011)

#### 4.4 Performance based Earthquake Engineering (PBEE) Seismic Slope Displacement Model:

“The procedure that has been used has been developed by Bray and Travararou(2009). This seismic slope displacement model enables one to estimate the potential seismic displacement (D) in centimeters.

$$\ln(D) = -1.10 - 2.83 \ln(k_y) - 0.333 (\ln(k_y))^2 + 0.566 \ln(k_y) \ln(S_a) + 3.04 \ln(S_a) - 0.244 (\ln(S_a))^2 + 1.5 T_s + 0.278 (M - 7) + \epsilon$$

where  $k_y$  = Yield constant.

$T_s$  = initial fundamental period of the sliding mass in seconds.

$T_s = \frac{4H}{V_s}$  where  $V_s$  = average shear wave velocity of the sliding mass.

$S_a$  = 5% damped elastic spectral acceleration of the sites design ground motion at a period of  $1.5 T_s$  in unit of g.

$M$  = magnitude of Earthquake.

$\epsilon$  = normally distributed random variable with zero mean and standard deviation ( $\sigma$ ) = 0.66.

If  $T_s < 0.05s$ , the first term ( i.e., -1.10 is replaced by -0.22.

Bray and Travararou developed the method for calculating seismic coefficient for the slope displacement model by the following equations:

$$k = \exp\left[\frac{-a + \sqrt{b}}{0.665}\right]$$

where  $a = 2.83 - 0.566 \ln(S_a)$

$$b = a^2 - 1.33 [\ln(D_a) + 1.10 - 3.04 \ln(S_a) + 0.244 (\ln(S_a))^2 - 1.5 T_s + 0.278 (M - 7) + \epsilon]$$

$D_a$  = allowable seismic displacement in centimeters, the percent exceedance of this displacement threshold is required for the calculation of  $\epsilon$  for example for 50% exceedance level  $\epsilon = 0$ .” (Bray, 2011)

“The design spectral acceleration is calculated ground motion models in a deterministic seismic hazard assessment (DSHA) or Probabilistic Seismic Hazard Assessment (PSHA). The spectral acceleration is dependent o factors like source to site distance, Earth quake magnitude, site conditions, topographic effect, etc.” (Bray, 2011)

**Faults that have been considered:**

The faults that have been considered for the calculation of design spectral acceleration by the process of DSHA and PSHA are as follows Balapur fault, MBT, Raithan fault, Zanskar thrust, F81.

For calculation of design spectral acceleration the method that has been used is “Rao” method. For the calculation of Peak ground acceleration (PGA) in the units of ‘g’ Rmin(minimum distance of fault from the study area), Mmax(maximum magnitude that can be generated by the fault), depth of the fault in meters, Hypocentral distance are required. The formulas that have been used are as follows:

Wells and Coppersmith (1994) relation of moment magnitude with subsurface rupture length (RLD) has been used

$$\text{Magnitude (Mw)} = 5.5 + 1.22 * \log(\text{length of fault})$$

$$\text{Log(PGA)} = C1 + C2(Mw-6) + C3(Mw-6)^2 + C4 *(R) + C5 \text{Log}(E)$$

Where PGA is in the values of “g”, Mw is the maximum magnitude generated by the fault , E is the Hypocentral distance and C1,C2,C3,C4,C5 are constants having values as:

$$\begin{aligned} C1 &= 0.66845 & C2 &= 0.49908 & C3 &= -0.04665 \\ C4 &= -0.00257 & C5 &= -0.85968 & \sigma(\log(E)) &= 0.1118 \end{aligned}$$

$$\text{Hypocentral distance} = \sqrt{R * H + H * H} \quad \text{where H is the depth of fault in km.}$$

“The latitudes and longitudes of various points along the length of the faults that were considered in the study were found out and by the Great Circle Distance formula distance between different points was calculated. Also distance of the fault from the site under consideration that is the centre of Srinagar city was calculated using the same formula. For DSHA only R<sub>min</sub> that is the minimum distance of fault from the site is considered.

$$\text{Formula for calculating distance between two latitude, longitude} = \cos^{-1}(\cos(90 - \text{longitude}(1)) * \cos(90 - \text{longitude}(2)) * \sin(90 - \text{longitude}(2)) * \sin(90 - \text{longitude}(1)) * \cos(\text{latitude}(2) - \text{latitude}(1))) * (\text{radius of earth(km)}))$$

Formula for calculating distance from site to the fault:

=  $\cos^{-1}(\cos(90-\text{longitude of centre of study area}) * \cos(90-\text{logitude}(2)) * \sin(90-\text{longitudeof centere of study area}) * \sin(90-\text{longitude})) * \cos(\text{latitude of centre of study area}-\text{latitude}(1))) * (\text{radius of earth}(\text{km}))$ .” (Bray, 2011)

**Table 4.5: Peak ground acceleration calculations for different faults.**

Fault no	Fault name	Rmin	Mw	Depth	Hypocentral distance	Pga(Sa/g) Rao
1	MBT	54.228	8.356	30	61.9731	0.7828
2	Balapur Fault	23.448	7.204	30	38.0763	0.5666
3	Raithan Fault	18.251	6.431	30	35.1155	0.2913
4	Zankskar thrust	100.064	7.849	30	104.464	0.2728
5	F35	35.902	6.811	30	46.7862	0.3125

#### Calculation of Shear wave velocity:

We need to calculate the shear wave velocity for the calculation of the Fundamental period of the time and the equations that have been used are as follows:

$$\frac{V_p}{V_s} = \sqrt{\frac{1-\gamma}{0.5-\gamma}}$$

where  $V_p$  is the compression wave velocity.

$\gamma$  is the Poisson's ratio,  $V_s$  is the shear wave velocity.

$$V_p = \sqrt{\frac{M}{\rho}}$$

where  $M$ = constrained modulus and  $\rho$ = mass density.

Then after the calculation of  $V_s$  we can calculate  $T_s$  in seconds by the equation

$$T_s = \frac{4H}{V_s}$$

where  $H$  is the representative height in this case 300m.

**Table 4.6: Unit weights for different rocks at site.**

Type of rock	$\rho$ (N/mm <sup>2</sup> )
Phyllitic Quartzite	26.87*10 <sup>-6</sup>
Quartzitic Phyllite	25.99*10 <sup>-6</sup>
<b>T</b> <b>a</b> <b>b</b> <b>l</b> <b>e</b> Siltstone	25.99*10 <sup>-6</sup>
Granodiorite	26.68*10 <sup>-6</sup>

**Table 4.7: Shear wave velocity calculations.**

E( GPa)	$\Gamma$	$\sqrt{\frac{1-\gamma}{0.5-\gamma}}$	Vp(m/s)	Vs(m/s)	Ts (s)
70.7	0.19	1.616	51295.099	3174.1	0.378
14.9	0.22	1.66	23943.6	1442.3	0.832
42.1	0.17	1.55	40247.40	2539.24	0.472
62.9	0.15	1.585	48554.82	3132.5	0.383

After the calculation of shear wave velocity (m/s), initial fundamental period of sliding mass (s) and peak ground acceleration, the Pseudo static analysis is being carried out. The results are obtained in the form of a relationship between seismic coefficient that is corresponding to a particular allowable displacement and seismic slope stability parameters. Allowable displacement of 5, 15, and 30 centimeters have been used so as to show dependence of seismic coefficient on it. The observations that were made are as follows:[1] Seismic Coefficient increases with the increase in ground motion intensity.[2]It increases as

magnitude (duration) of earthquake increases. [3]It significantly decreases as the allowable displacement increases.

**Table 4.8: Seismic coefficient calculations for D=5cm, Ts = 0.378**

D= 5cm	Ts=0.378	M=7.8				
Sa	A	a*a	X	B	√b	$k=\exp(-a+\sqrt{b})/0.665$
0	0	0	0	0	0	0
0.5	3.222	10.38	5.52	4.86	2.204	0.217
0.78	2.97	8.82	3.578	5.242	2.289	0.359
1	2.83	8	2.553	5.447	2.333	0.4736
1.25	2.703	7.306	1.667	5.639	2.374	0.609
2	2.437	5.938	-0.0929	6.03	2.45	1.019
2.5	2.311	5.34	-878	6.218	2.49	1.028

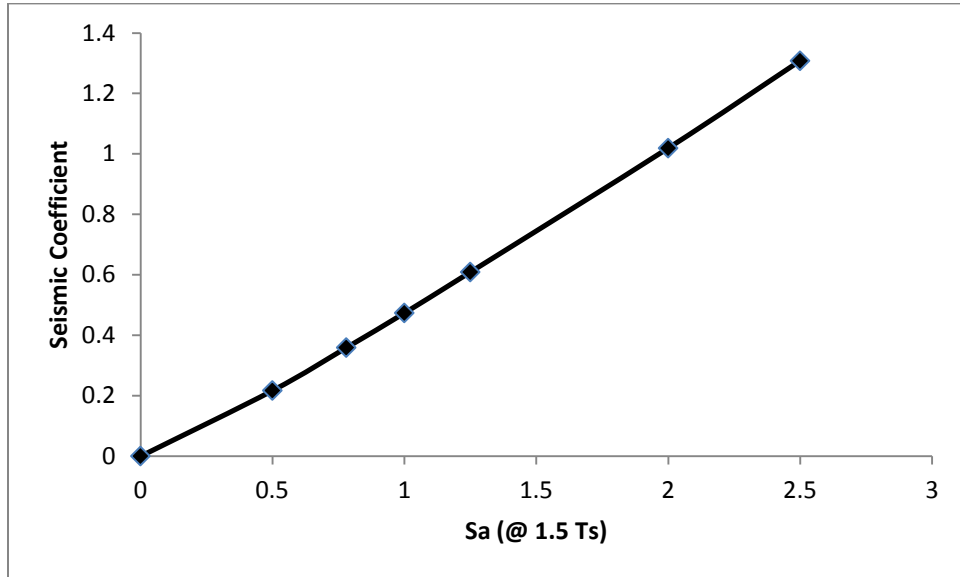
**Table 4.9: Seismic coefficient calculations for D=15cm, Ts= 0.378**

D=15cm	Ts=0.378	M=7.8				
Sa	A	a*a	x	b	√b	$k=\exp(-a+\sqrt{b})/0.665$
0	0	0	0	0	0	0
0.5	3.222	10.38	6.973	3.407	1.845	0.126
0.78	2.97	8.82	5.039	3.781	1.944	0.213
1	2.83	8	4.014	3.986	1.996	0.285
1.25	2.703	7.306	3.128	4.178	2.044	0.371
2	2.437	5.938	1.368	4.57	2.137	0.636
2.5	2.311	5.34	0.582	4.758	2.181	0.822

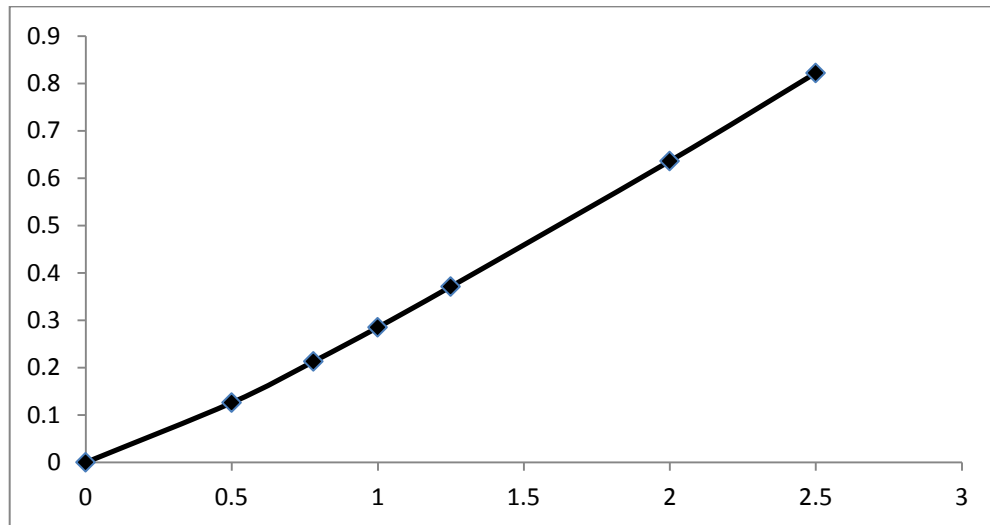
**Table 4.10 Seismic coefficient calculations for D=30cm, Ts=0.378**

D=30cm	Ts=0.378	M=7.8				
Sa	A	a*a	X	b	√b	$k=\exp(-a+\sqrt{b})/0.665$
0	0	0	0	0	0	0
<b>P</b> 0.5	3.222	10.38	7.895	2.485	1.576	0.084
<b>l</b> 0.78	2.97	8.82	5.96	2.86	1.691	0.146
<b>o</b> 1	2.83	8	4.936	3.064	1.75	0.197
<b>t</b> 1.25	2.703	7.306	4.05	3.256	1.804	0.258
<b>t</b> 2	2.437	5.938	2.29	3.648	1.9	0.445
<b>t</b> 2.5	2.311	5.34	1.504	3.836	1.958	0.588

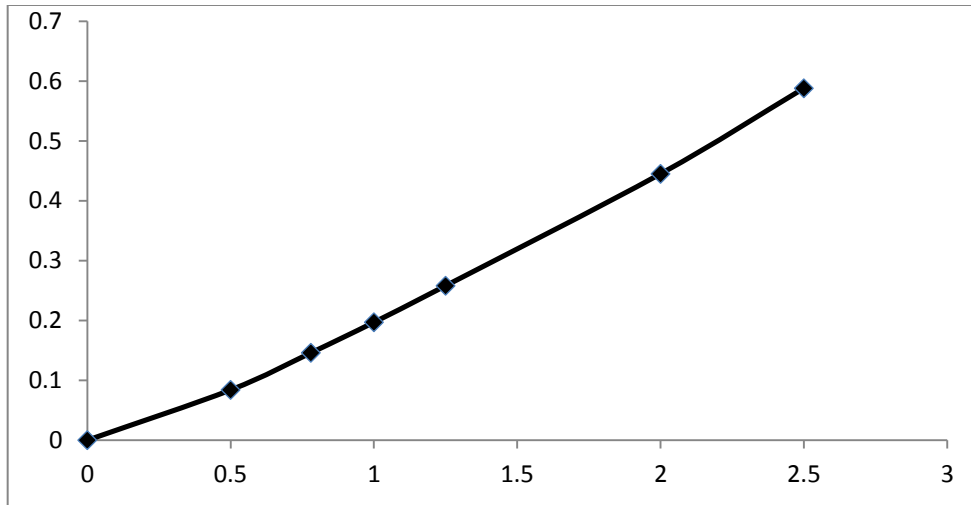




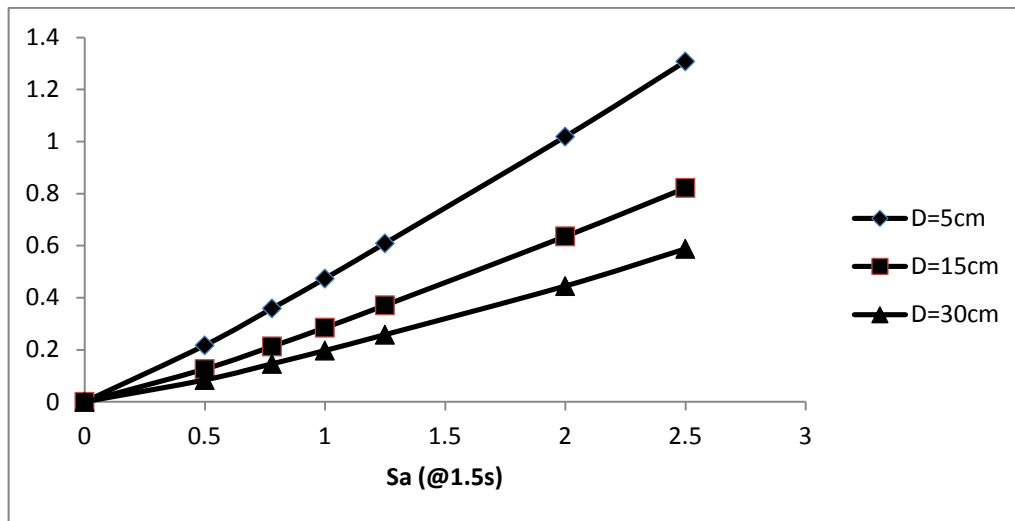
**Graph 4.4 : Variation of seismic coefficient with peak ground acceleration (D=5cm),Ts=0.378**



**Graph 4.5: Variation of seismic coefficient with peak ground acceleration (D=15cm),Ts=0.372**



**Graph 4.6: Variation of seismic coefficient with peak ground acceleration (D=30cm),  $T_s=0.372$**



**Graph 4.7: Combined variation of seismic coefficient with peak ground acceleration,  $t_s=0.372$**

From the graphs it is evident that with the increase of the peak ground acceleration there is an increase of the specific coefficient. And as the displacement(D) increases there is an increase of the seismic coefficient.

**Table 4.11: Seismic coefficient calculations for D=5cm, Ts=0.472**

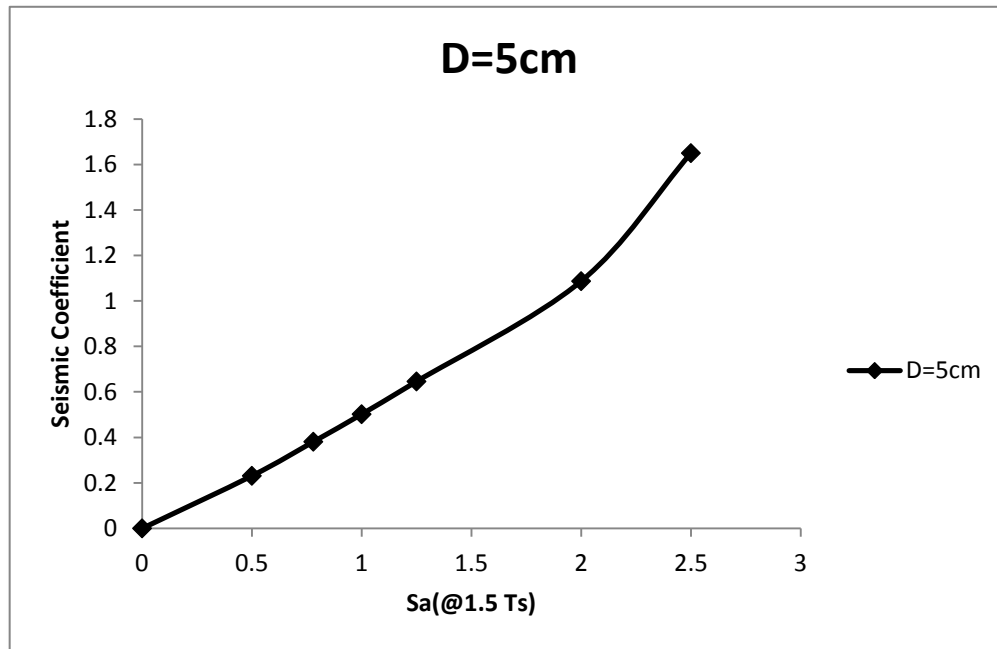
<b>D=5cm</b>	<b>Ts=0.472</b>	<b>M=7.8</b>				
Sa	a	a*a	x	b	√b	$k=\exp(-a+\sqrt{b})/0.665$
0	0	0	0	0	0	0
0.5	3.222	10.38	5.324	5.056	2.248	0.231
0.78	2.97	8.82	3.39	5.43	2.33	0.381
1	2.83	8	2.366	5.634	2.373	0.502
1.25	2.703	7.306	1.48	5.826	2.413	0.646
2	2.437	5.938	-0.28	6.218	2.493	1.087
2.5	2.311	5.34	-1.066	7.004	2.646	1.65

**Table 4.12: Seismic coefficient calculations for D=15cm, Ts=0.472**

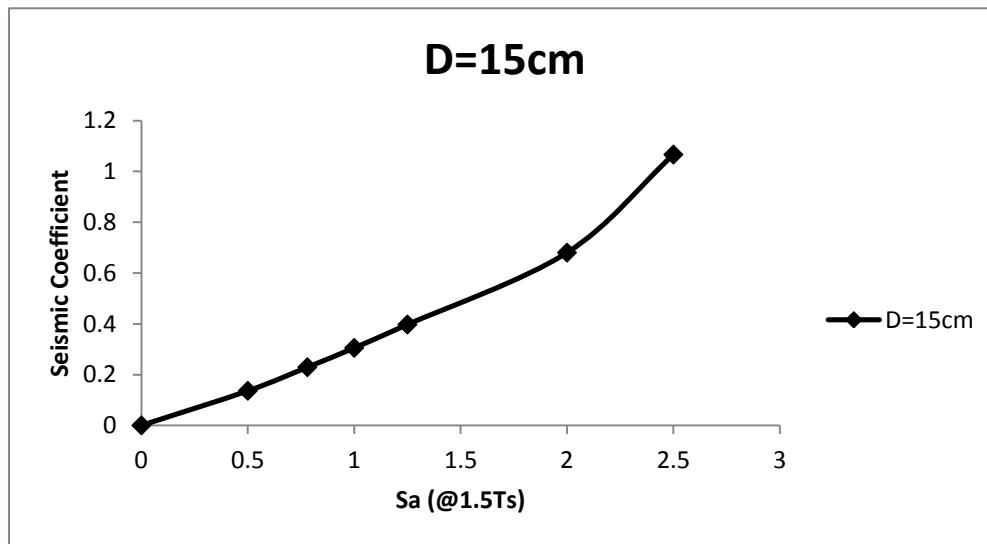
<b>D=15cm</b>	<b>Ts=0.472</b>	<b>M=7.8</b>				
Sa	A	a*a	x	b	√b	$k=\exp(-a+\sqrt{b})/0.665$
0	0	0	0	0	0	0
0.5	3.222	10.38	6.785	3.595	1.896	0.136
0.78	2.97	8.82	4.851	3.969	1.992	0.229
1	2.83	8	3.827	4.173	2.042	0.305
1.25	2.703	7.306	2.941	4.365	2.089	0.397
2	2.437	5.938	1.18	4.758	2.181	0.68
2.5	2.311	5.34	0.394	5.544	2.354	1.066

**Table 4.13: Seismic coefficient calculations for D=30cm, Ts=0.472**

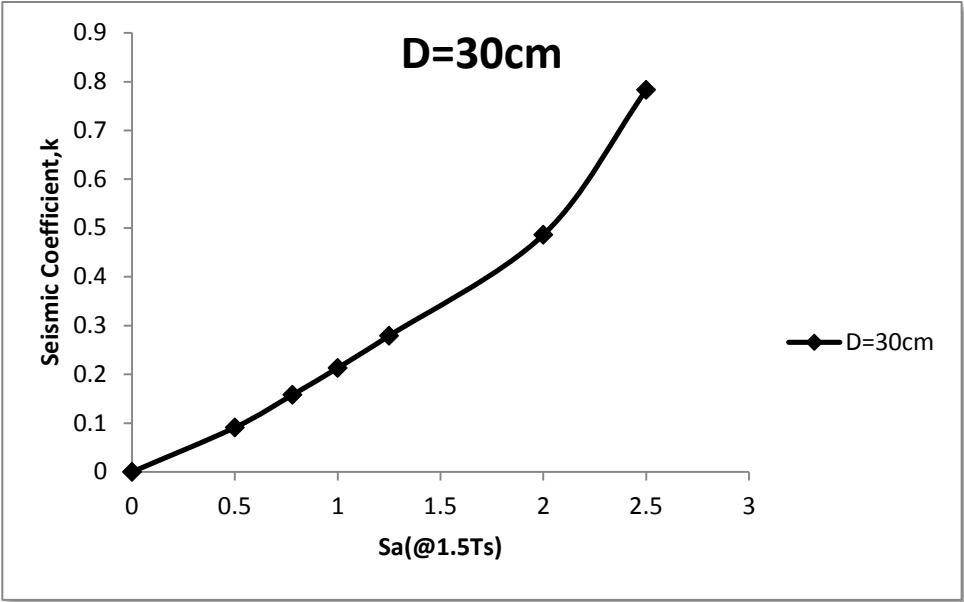
<b>D=30cm</b>	<b>Ts=0.472</b>	<b>M=7.8</b>				
Sa	A	a*a	x	b	√b	$k=\exp(-a+\sqrt{b})/0.665$
0	0	0	0	0	0	0
0.5	3.222	10.38	7.707	2.673	1.634	0.091
0.78	2.97	8.82	5.773	3.047	1.745	0.158
1	2.83	8	4.749	3.251	1.803	0.213
1.25	2.703	7.306	3.863	3.443	1.855	0.279
2	2.437	5.938	2.102	3.835	1.958	0.486
2.5	2.311	5.34	1.316	4.622	2.149	0.783



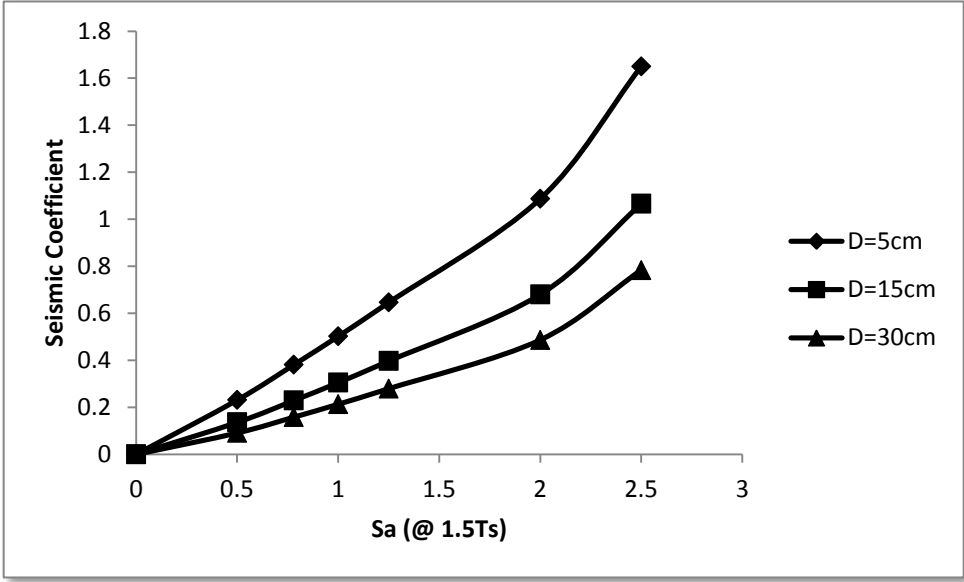
**Graph4.8:** Variation of seismic coefficient with peak ground acceleration (D=5cm), $T_s=0.472$



**Graph 4.9:** Variation of seismic coefficient with peak ground acceleration (D=15cm), $T_s=0.472$



Graph 4.10: Variation of seismic coefficient with peak ground acceleration (D=30cm), Ts=0.472



graph 4.11: Combined variation of seismic coefficient with PGA, Ts=0.472

**Table 4.14: Seismic coefficient dependence on fundamental period of sliding mass (D=5cm)**

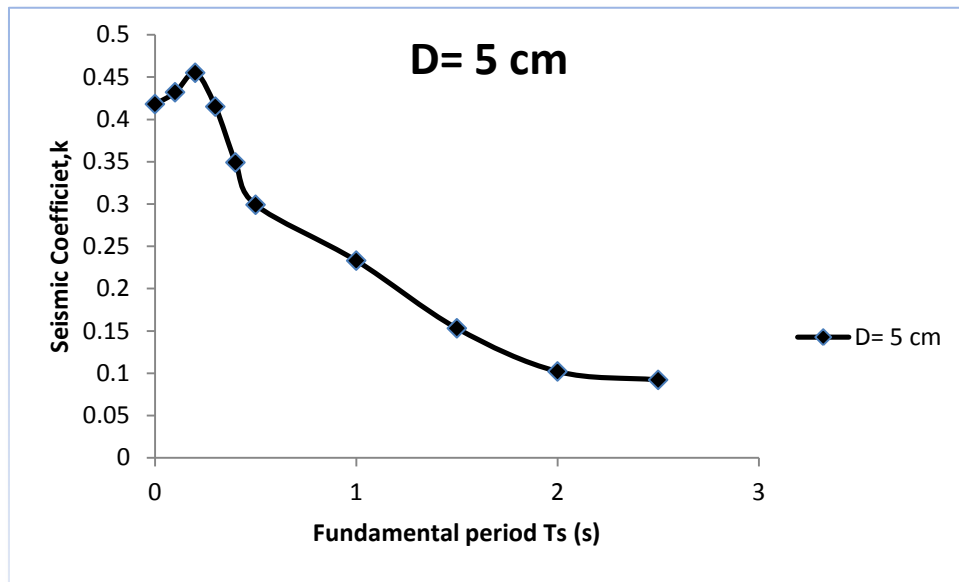
D=5cm M=7.8	a=3.009 a*a=9.058	Sa=.782g Fault name: Main Boundary Thrust	$\sqrt{b}$	$k=\exp(-a+\sqrt{b})/0.665$
Ts	x	B		
0	3.151	5.907	2.43	0.418
0.1	3.129	5.929	2.435	0.422
0.2	2.883	6.175	2.485	0.455
0.3	3.732	5.326	2.308	0.349
0.4	4.466	4.592	2.143	0.272
0.5	4.703	4.355	2.087	0.25
1	5.961	3.097	1.76	0.153
1.5	6.838	2.22	1.49	0.102
2	7.042	2.016	1.42	0.092
2.5	7.451	1.607	1.268	0.073

**Table 4.15: Seismic coefficient dependence on fundamental period of sliding mass (D=15cm)**

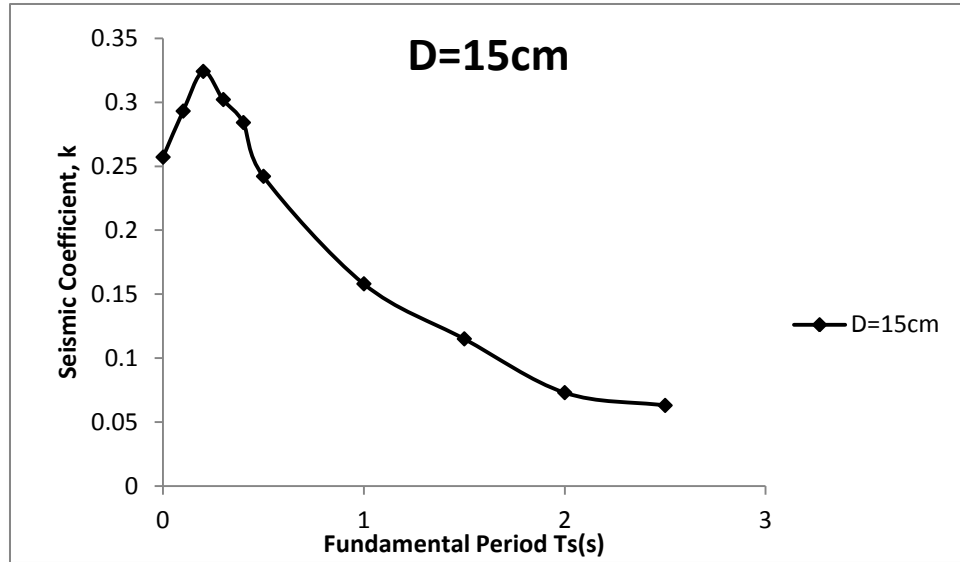
D=15cm M=7.8	a=3.009 a*a=9.058	Sa=.782g Fault name: Main Boundary Thrust	$\sqrt{b}$	$k=\exp(-a+\sqrt{b})/0.665$
Ts	x	b		
0	4.612	4.44	2.108	0.257
0.1	4.254	4.804	2.192	0.293
0.2	3.955	5.103	2.259	0.324
0.3	4.166	4.892	2.212	0.302
0.4	4.345	4.713	2.171	0.284
0.5	4.794	4.264	2.065	0.242
1	5.887	3.171	1.781	0.158
1.5	6.594	2.464	1.57	0.115
2	7.451	1.607	1.286	0.073
2.5	7.69	1.368	1.17	0.063

**Table 4.16: Seismic coefficient dependence on fundamental period of sliding mass (D=30cm)**

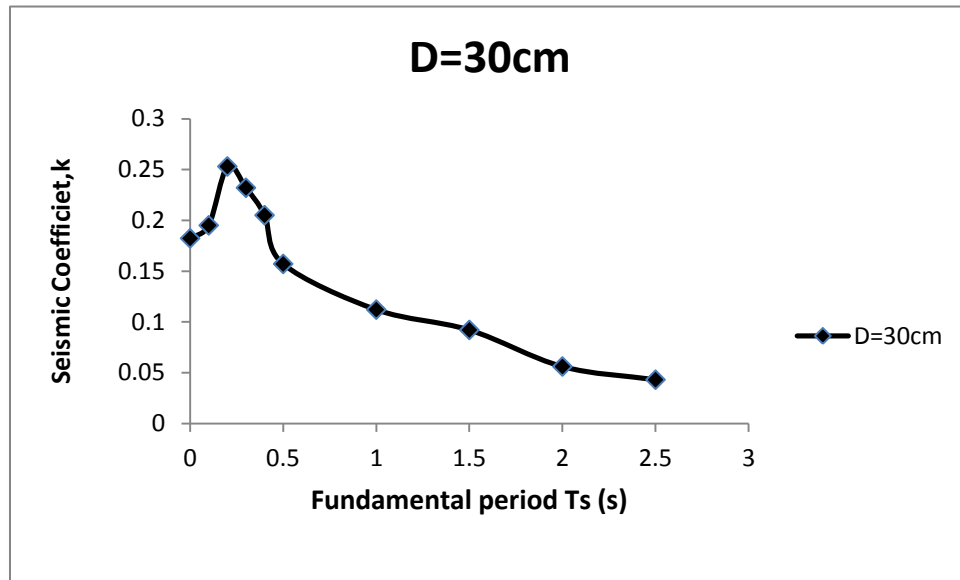
D=30cm	a=3.009	Sa=.782g		
M=7.8 Ts	a*a=9.058 X	Fault name: Main Boundary Thrust b	$\sqrt{b}$	$k=\exp(-a+\sqrt{b})/0.665$
0	5.534	3.523	1.877	0.1822
0.1	5.368	3.69	1.921	0.195
0.2	4.669	4.389	2.095	0.253
0.3	4.909	4.149	2.037	0.232
0.4	5.236	3.822	1.955	0.205
0.5	5.901	3.157	1.777	0.157
1	6.647	2.411	1.553	0.112
1.5	7.036	2.022	1.422	0.092
2	7.866	1.192	1.092	0.056
2.5	8.219	0.839	0.916	0.043



**Graph 4.12: Variation of seismic coefficient with fundamental period (D=5cm)**

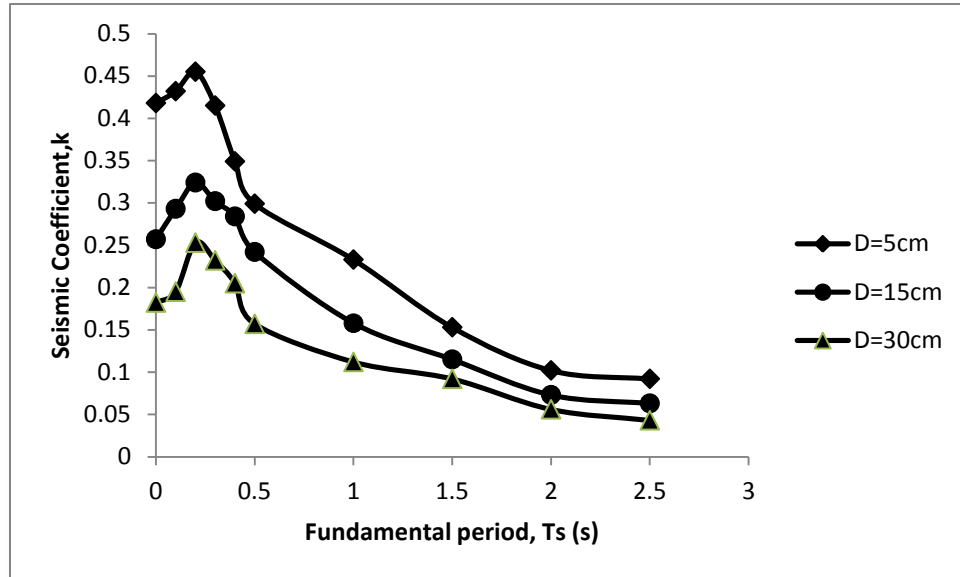


**Graph 4.13: Variation of seismic coefficient with fundamental period (D=15cm)**



**Graph 4.14: Variation of seismic coefficient with fundamental period (D=30cm)**





**Graph 4.15: Combined variation of seismic coefficient with fundamental period (D=5cm)**

Sliding mass's fundamental period is also a term on which the seismic coefficient is dependent. The slopes that are stiff have that is those having short fundamental periods ( $0.1s < T_s < 0.3s$ ) are having resonance with vibrating ground and hence displace more. Flexible slopes ( $T_s > 0.5s$ ) have less seismic displacement potential. As the slopes period increases from zero (rigid sliding), the seismic coefficient increases till a peak is reached and then it decreases as slopes period moves from the resonance.

#### **4.5 SOFTWARE ANALYSIS USING GEOSTUDIO:**

Firstly for the software analysis that has been carried out certain parameters are needed like cohesion ( $c$ ) in kPa, unit weight of rocks in  $\text{KN/m}^3$  and angle of internal friction ( $\phi$ ) in degrees (for MOHR COULOMB analysis) and uniaxial compressive strength in kPa,  $m_i$ , GSI,  $D$  ( for HOEK BROWN analysis) along the depth of the site for a distance of 250m for which the analysis is being done. After carefully studying the bore-hole data for the site, rock profile along the depth has been prepared and the significant changes that occur in it have been noted down after certain intervals. This profile gives in depth details about

parameters like lithological descriptions, structural description ( the two are required for calculating GSI),  $m_i$ , GSI, cohesion and angle of internal friction( both “ $c$ ” and “ $\phi$ ” have been calculated from the equivalent Mohr Coulomb method and Hoek Brown method).

	LITHOLOGICAL DESCRIPTION	GSI	$m_i$	$c$ (kpa)	$\phi$ (degrees)
0					
	SILTSTONE	35	9	161.7	48.86
48					
	SILTSTONE/ PHYLLITIC CHARACTERISTICS	50	9	428	46.70
51					
	SILTSTONE	60	9	792.8	45.024
68.5					
	PHYLLITIC QUARTZITE ROCK	60	10	1997	45.997
70					
	SILTSTONE	60	9	792.8	45.02
109					
	SILTSTONE	70	9	2530	34.248
194					
	SILTSTONE	85	9	5021.7	34.629
250					

**Fig 4.4: Rock profile below the slope for a depth of 250m.**

**Table 4.17: Lithological and structural description of rocks at site.**

Depth in meters	Lithological description	Structural description.
0-48	Highly fractured boulders of gravels and sandstone.	Overburden.
48-51	Siltstone/ weathered iron stained, fractured, rocks of siltstone having phyllitic characteristics.	Highly fractured rock.
51-68.5	Thinly foliated / weathered/ jointed / iron stained/ silica intruded siltstone.	Fractured dip at 76°.
68.5-70	Highly fractured/ thinly foliated, iron stained/ weathered/ Phyllitic rock.	Fractured rock.
70-109	Fractured, iron stained, thinly foliated sitstone.	Fractured rock.
109-194	Grey colour, fine grained, foliated, quartz vein, intruded solid, meta siltstone, iron stained.	Bedrock
194-250	Fine grained, foliated, vein intruded, meta siltstone.	Bedrock.

**Geometry of the model:**

The slope at site has been represented in GEOSTUDIO by taking into consideration two different ratios of vertical distance to horizontal distances that is 1:2 and 1:3.

**Material input and various conditions at site:**

The data at hand is for a depth of about 250m at the site and there is presence of different types rocks having different geological conditions. It is difficult to show all this information in a single model as some of the rocks are for few meters and some are for hundreds of meters. In order to have better clarity, 4 models have been made and the F.O.S has been calculated in all the cases. In model 1 a depth of 50m has been considered and a length of 100m in 1:2 ratio and 150m in 1:3 ratio, similarly in model 4 depth of 250m has been considered and then length of 750m is considered for 1:3 ratio and 500m for 1:2 ratio.

## MATERIALS:

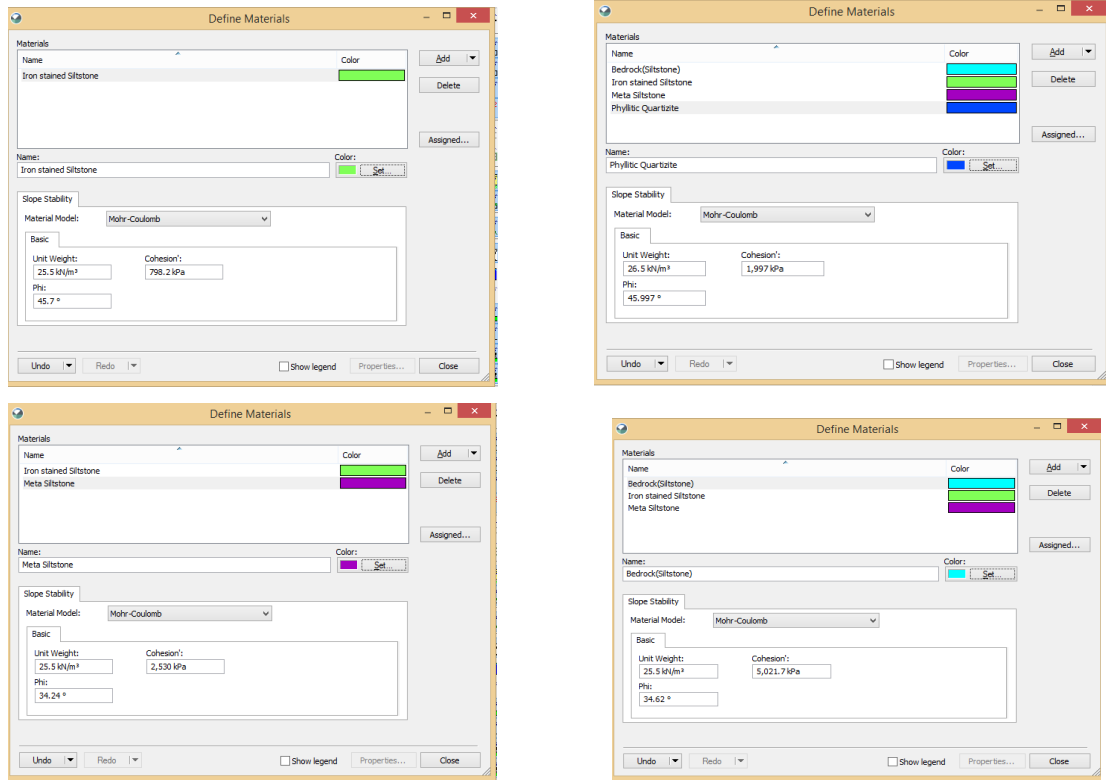


**Fig 4.5 : Input of the equivalent properties of  $c$ ,  $\gamma$  and  $\phi$ .**

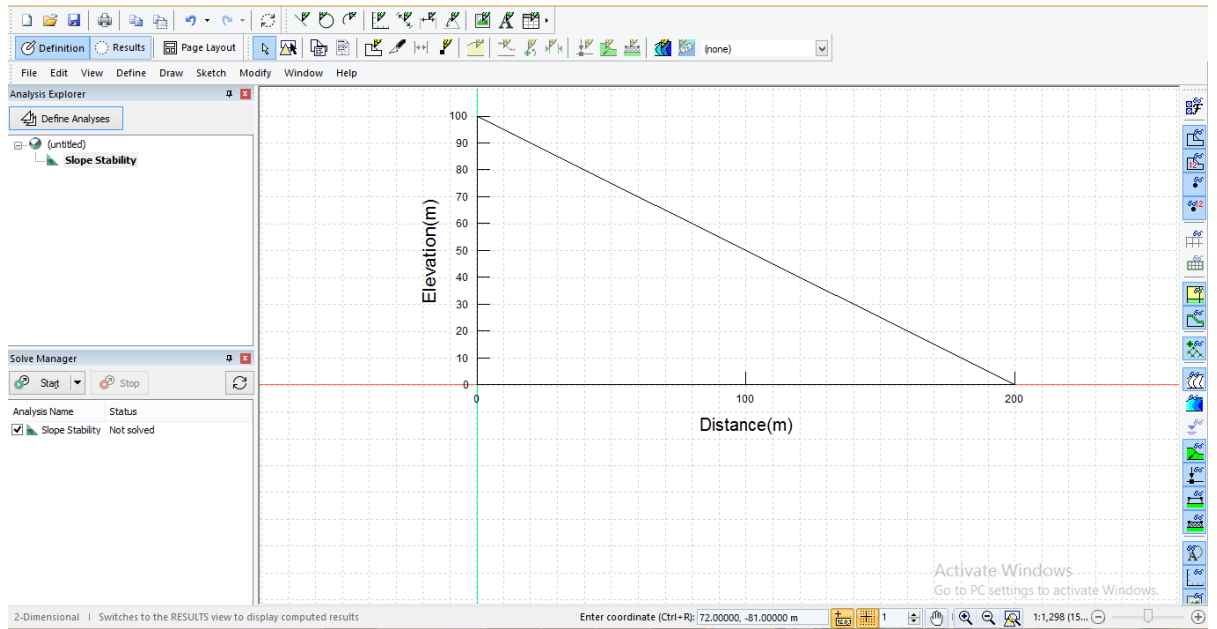


**Fig 4.6: Geometrical construction of the slope at site.**

Input the rock parameters, assign properties to the different layers at the site and define the geometry of the slope.

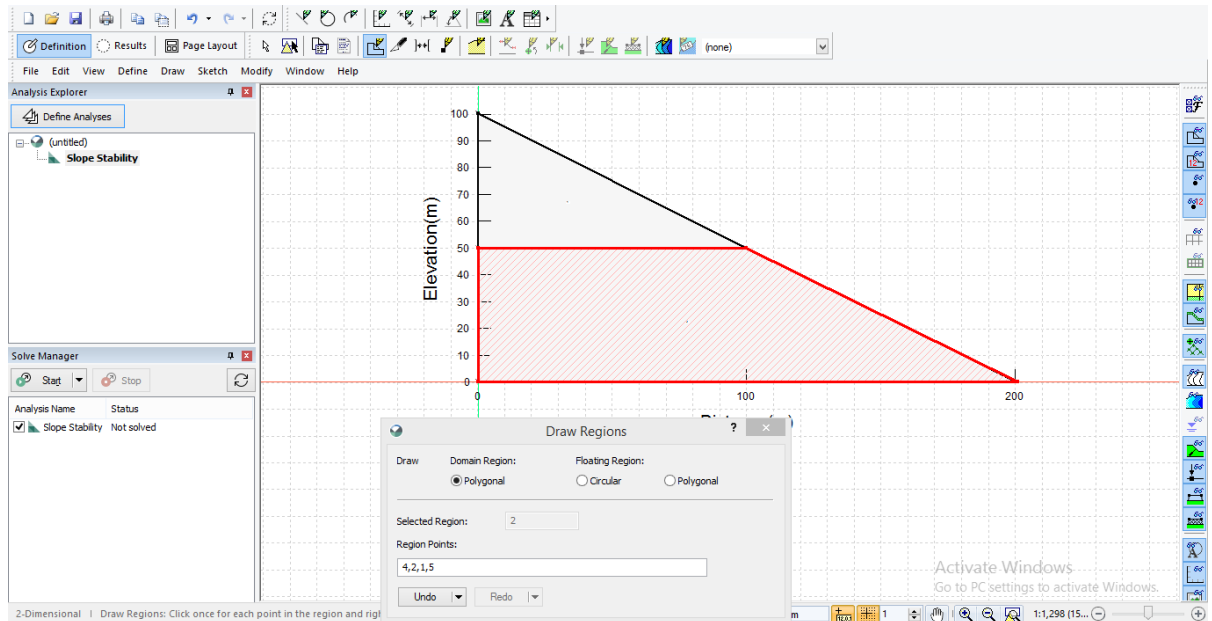


**Fig4.7 : Drawing of various regions.**

Different regions are firstly selected by looking into the bore-hole data logs. These regions are having different rock parameters like GSI, cohesion, frictional angle etc. After selection of regions the materials are input.

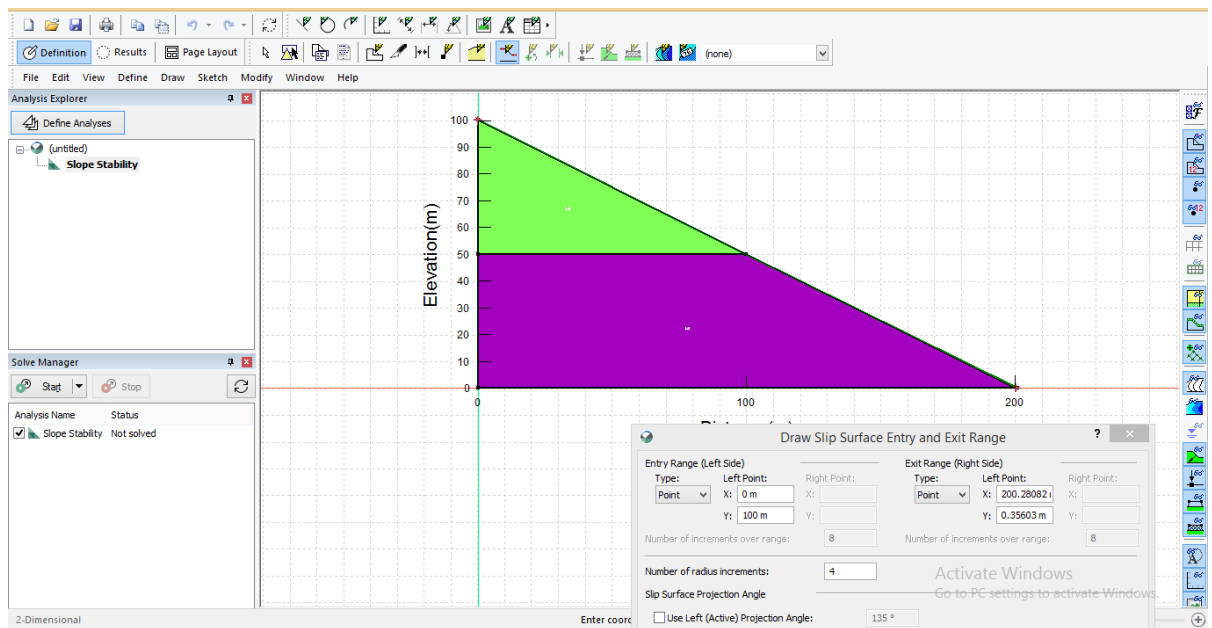
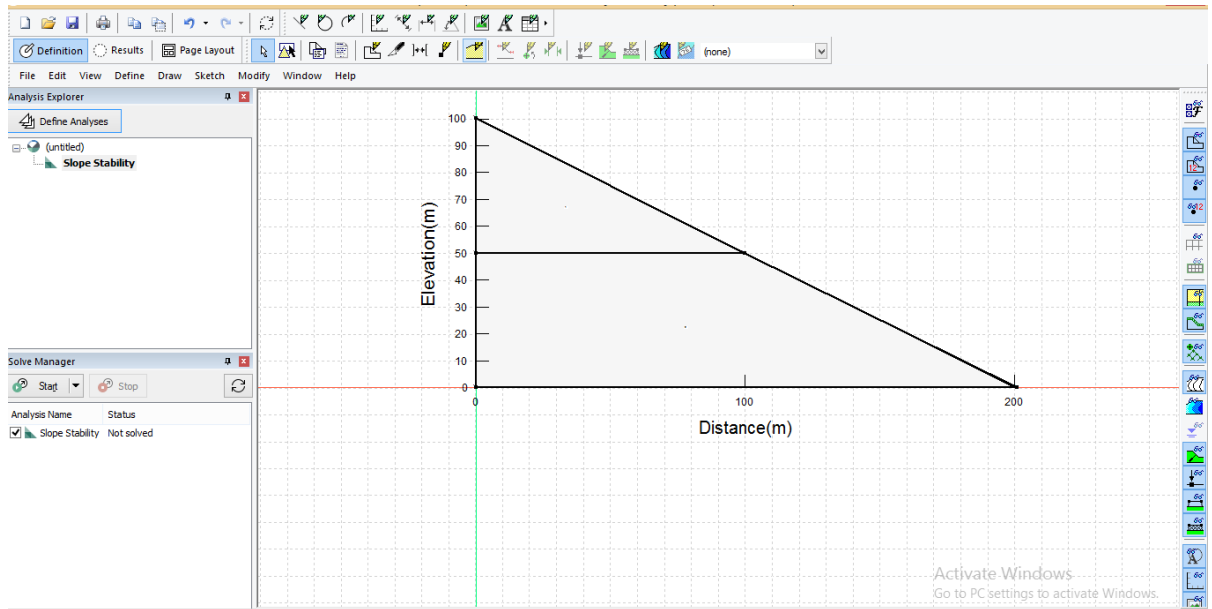


**Fig4.8 : Assigning the slip surface to the slope.**

The slip surface is drawn, in this case the entry and exit points are points. And after all this in the solve manager click on the start analysis to solve the slope stability problem and get a FOS and various graphs and body diagrams that are associated with it.

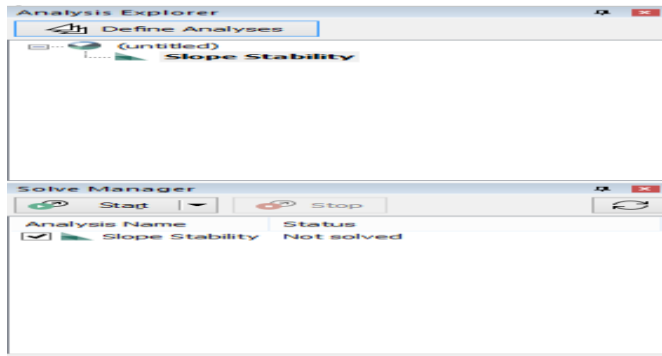


**Fig4.9 : Calculation stage.**

#### 4.6 RESULTS FROM SOFTWARE ANALYSIS:

Taking into consideration 50m in vertical direction and 100m in horizontal direction. There are two rock layers upper is that of siltstone and lower that of Phyllitic quartzite.

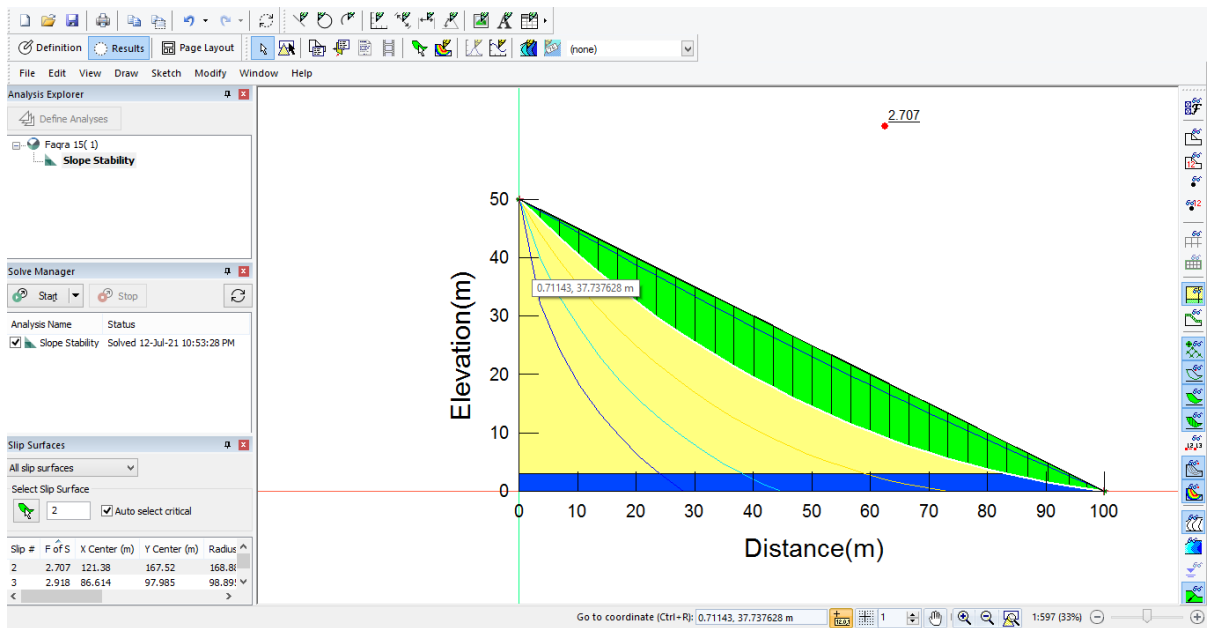


**Fig 4.10: F.O.S calculation and slip surface generation for 50m depth and 100m length.**

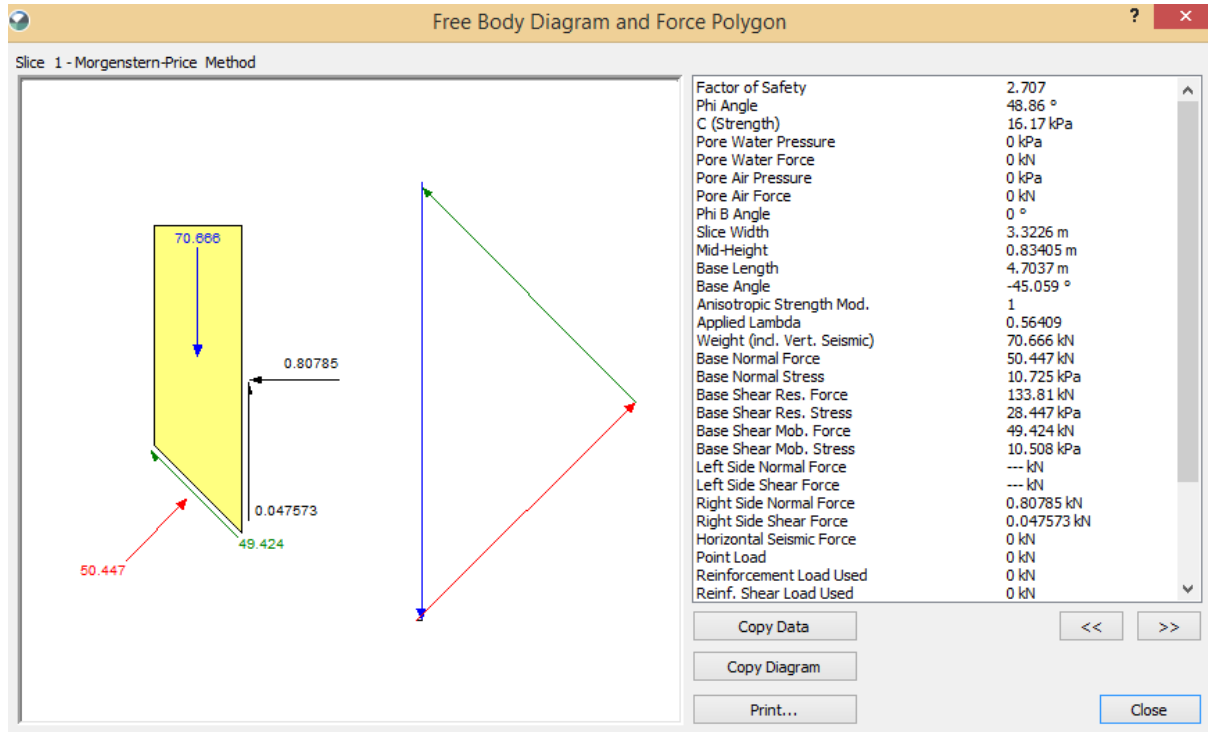


**Fig 4.11: Body diagram for the forces acting on the slope.**

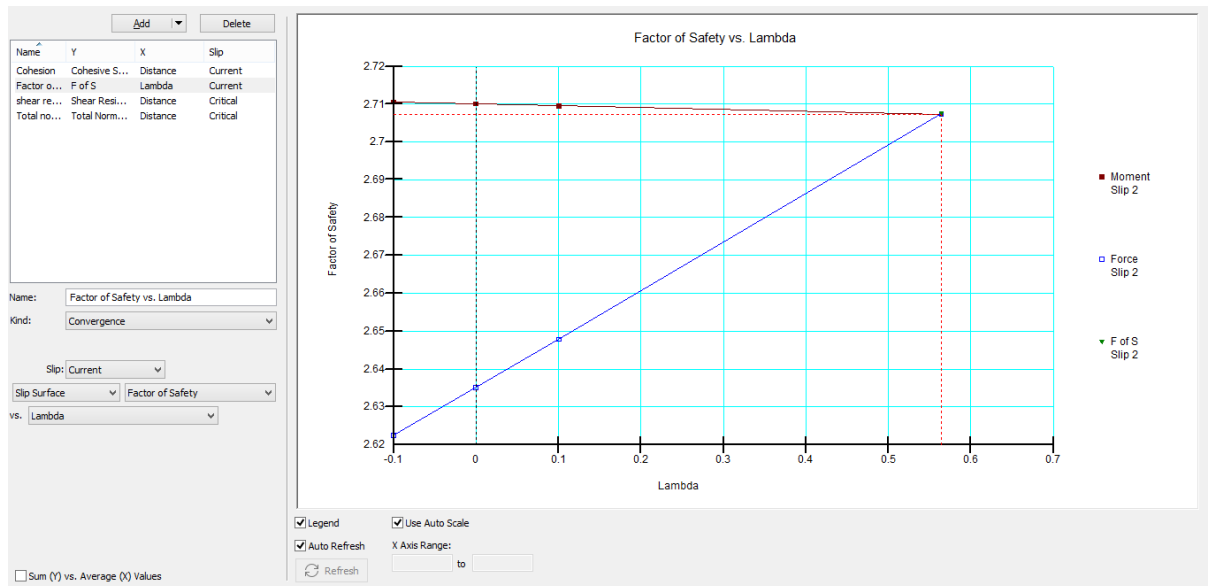


**Fig4.12: F.O.S vs Lambda.**

Morgenstern and Price method has been used for the analysis. In this method the software develops two factor of safety equations one with respect to the moment equilibrium and other with respect to horizontal force equilibrium. The interslice shear forces are handled with the help of equation proposed by Morgenstern



$X = E \lambda f(x)$  where  $f(x)$  is a function,  $\lambda$  (lambda) is the percentage of the function used in decimal form,  $E$  is the interslice normal force and  $X$  is the interslice shear force.

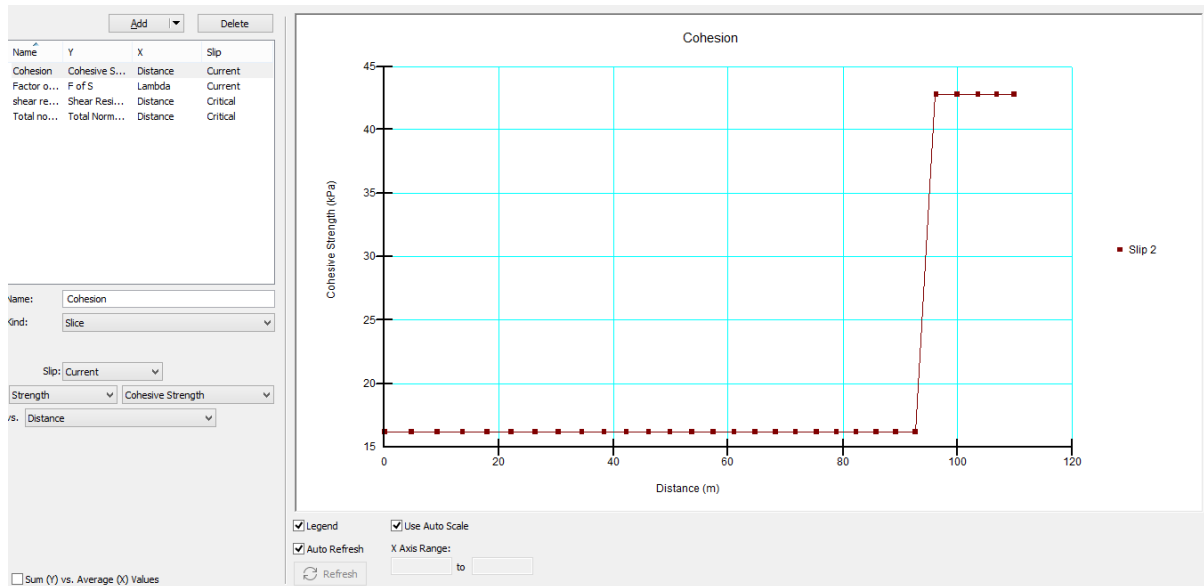


**Fig 4.13: Variation of cohesion along the distance( horizontal).**

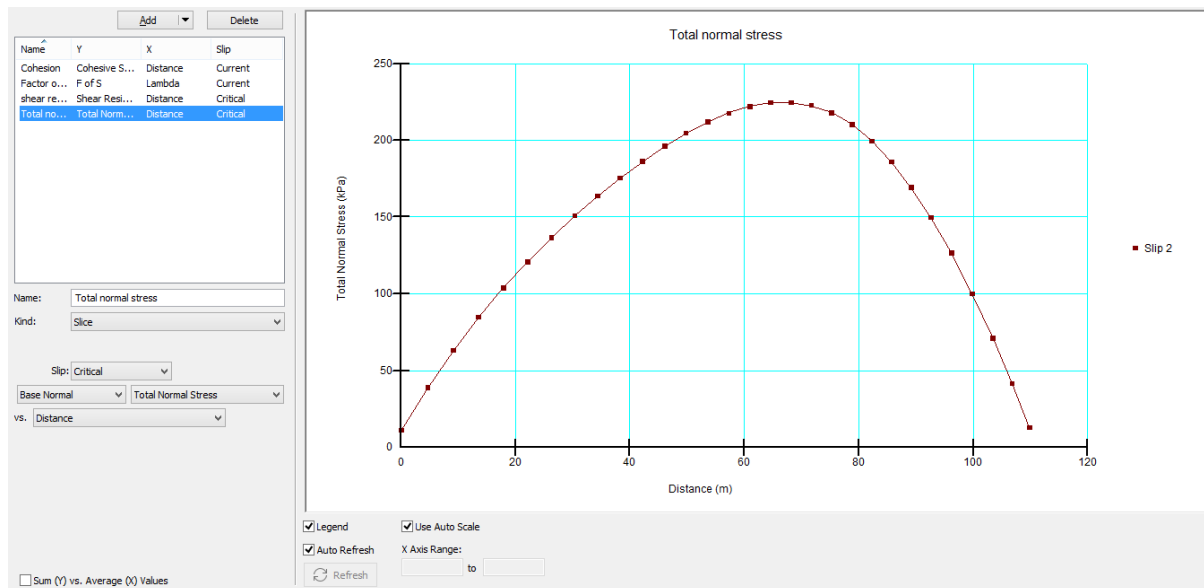


**Fig 4.14: Variation of Total normal stress along the distance (horizontal).**

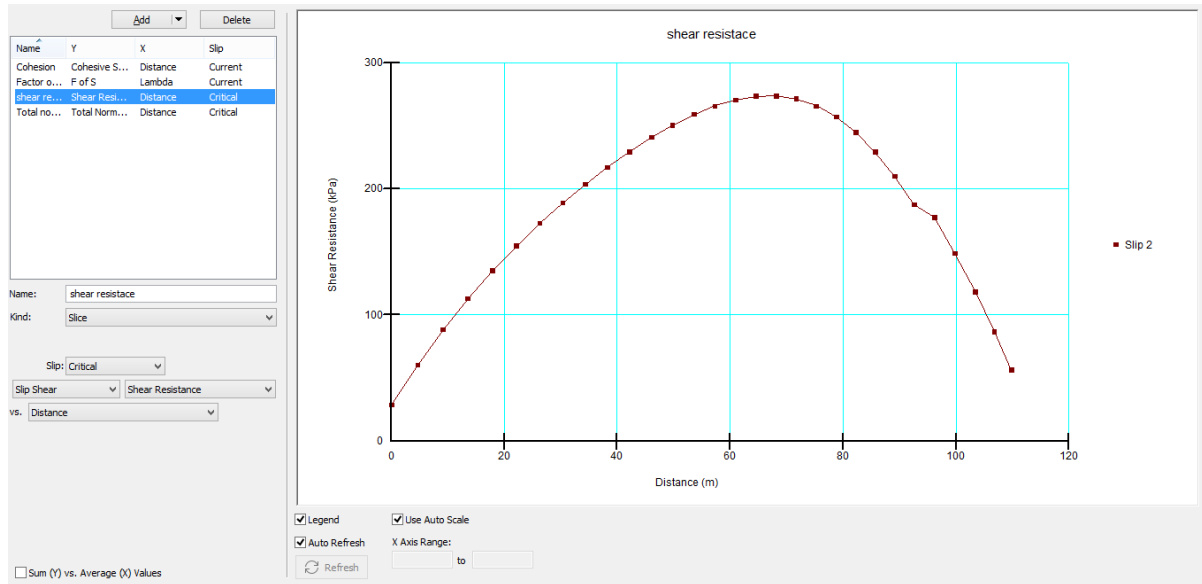


**Fig4.15: Variation of shear resistance along the distance ( horizontal).**

Taking into consideration three layers of rocks first that of siltstone, second is phyllitic quartzite, and the siltstone again. Vertical distance is 100m and horizontal is 200m.

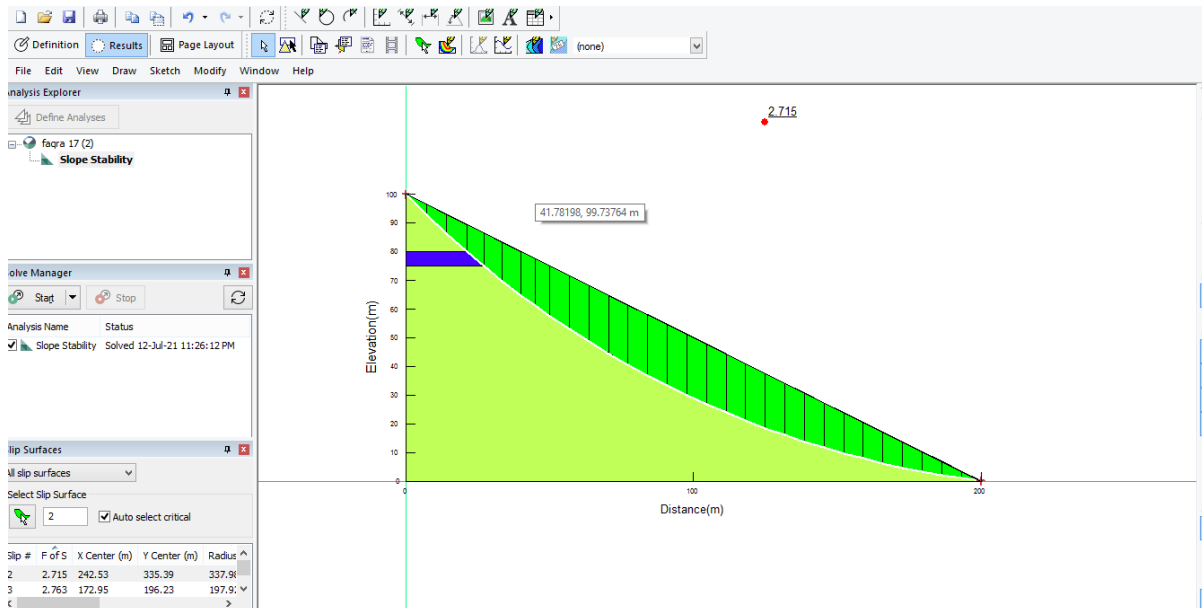


**Fig 4.16: F.O.S calculation and slip surface generation for 100m depth and 200m length.**

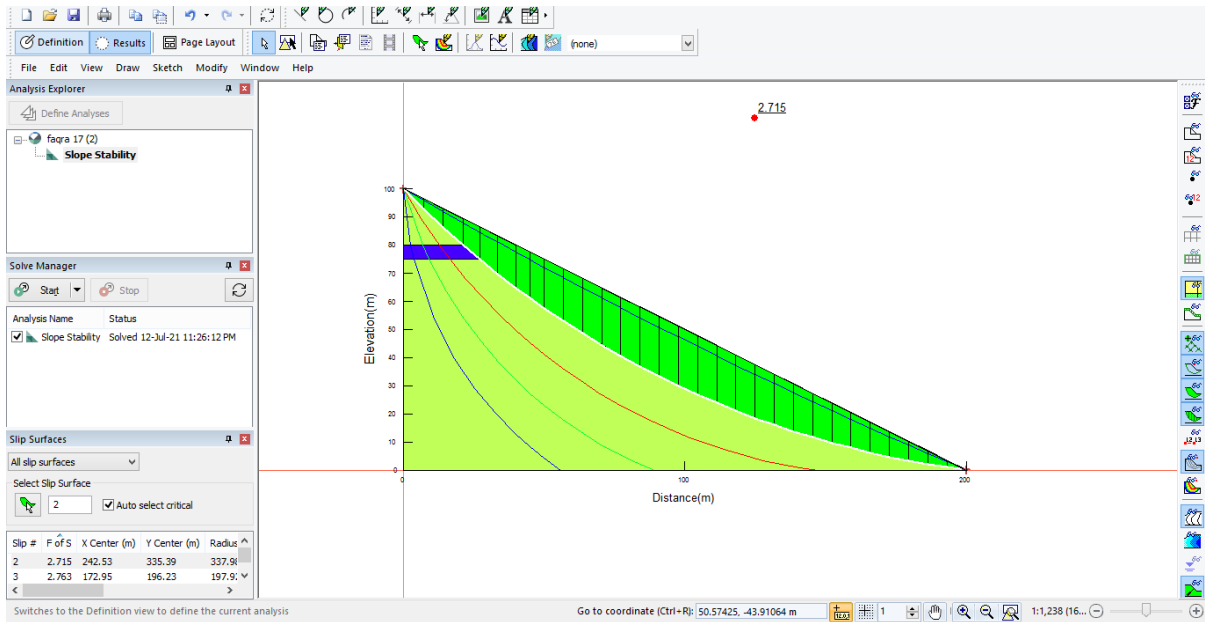


**Fig 4.17: F.O.S calculation and slip surface generation for 50m depth and 100m length showing all the slip surfaces.**

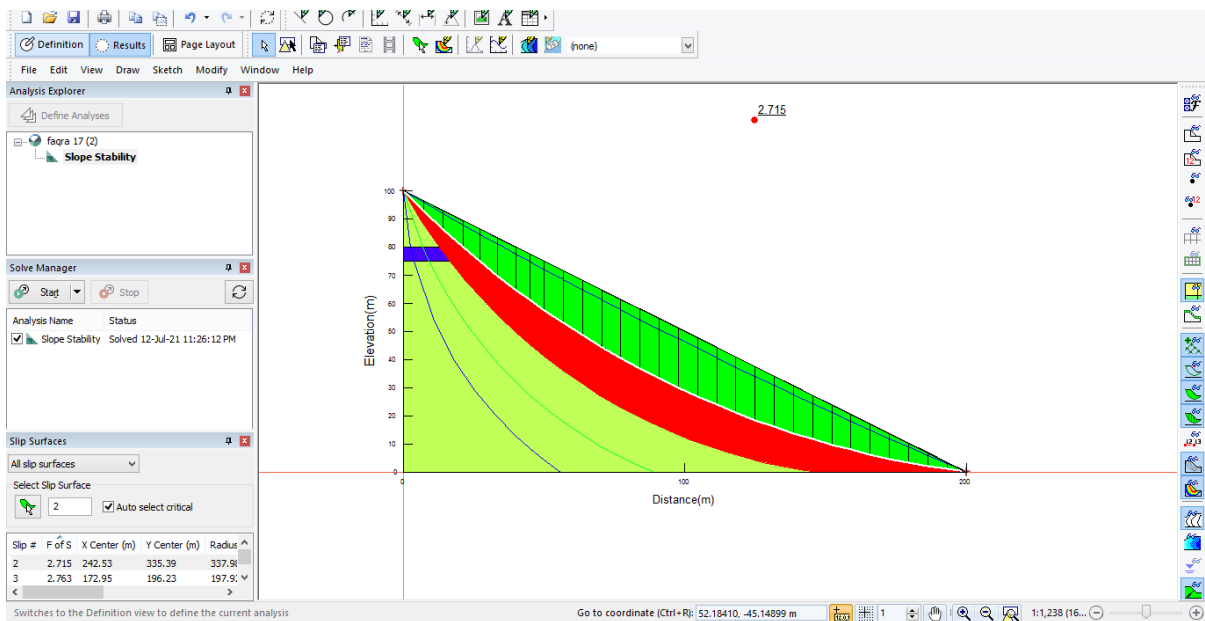


**Fig 4.18: F.O.S calculation and slip surface generation for 50m depth and 100m length showing the safety map zone.**

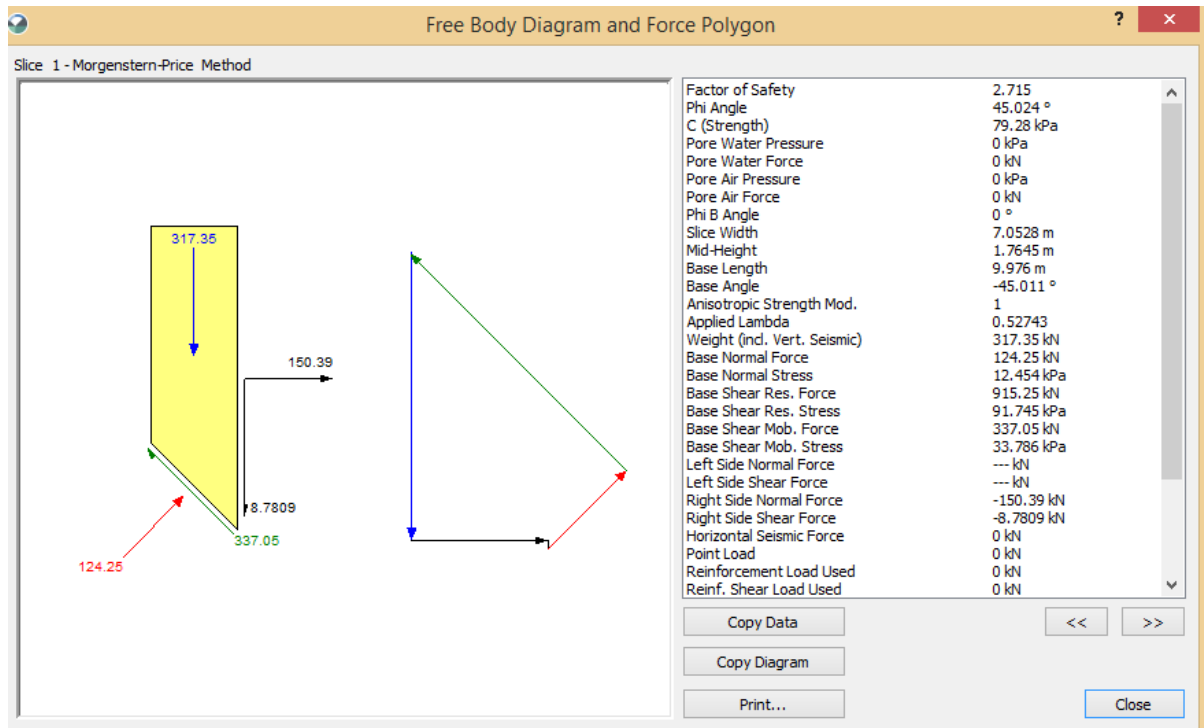


Fig 4.19: Body diagram for the forces acting on the slope.

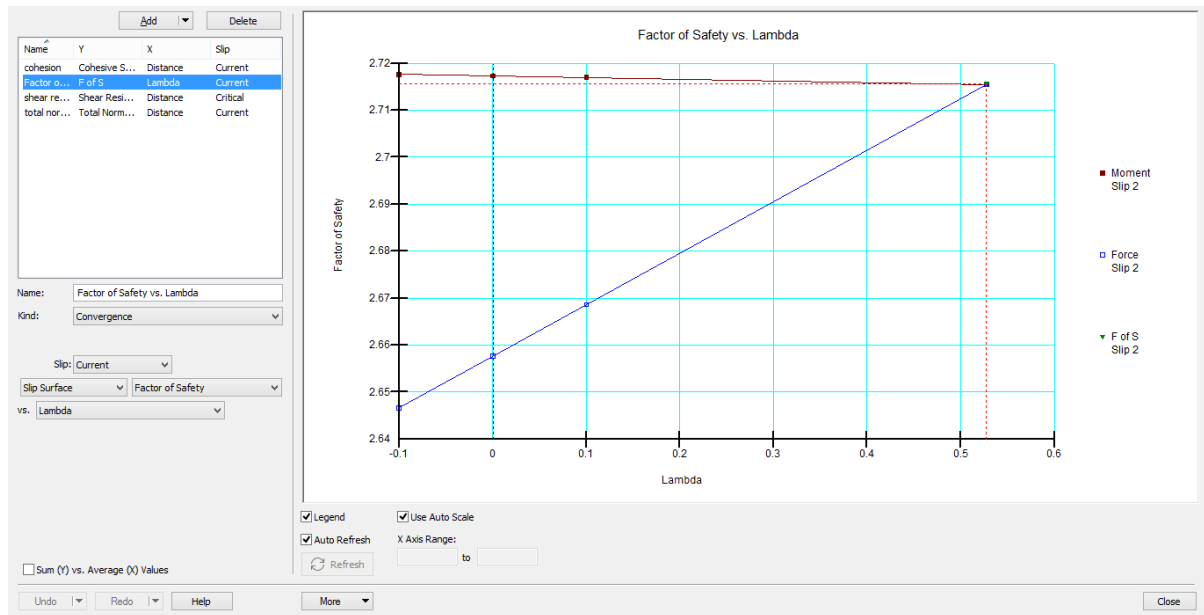
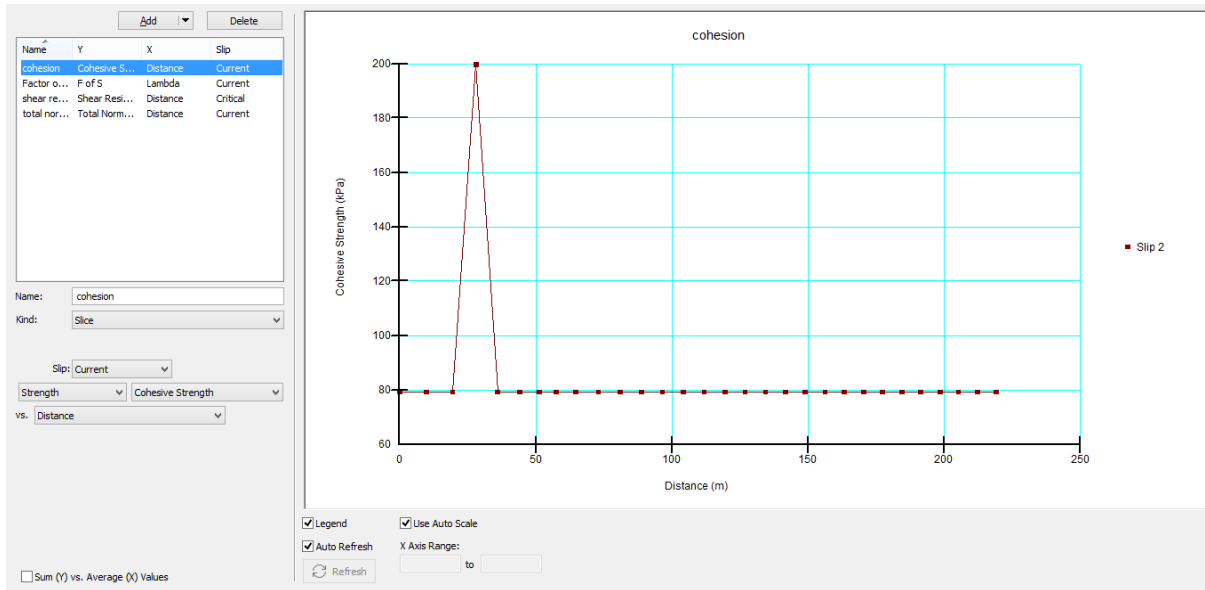
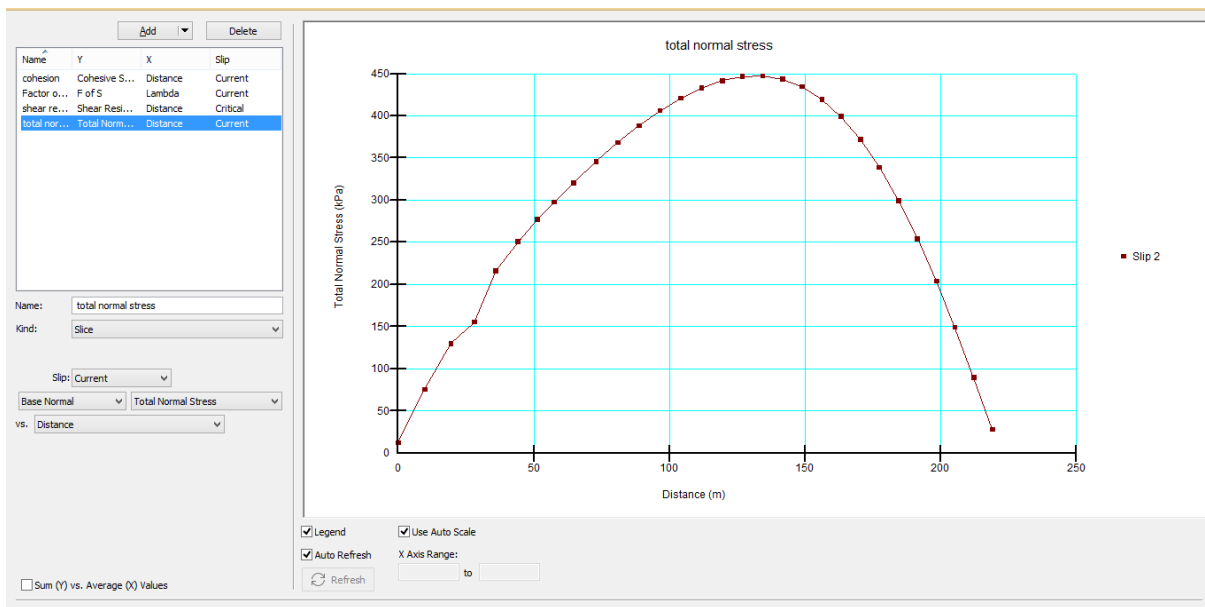


Fig4.20: F.O.S vs Lambda.



**Fig 4.21: Variation of cohesion along the distance( horizontal).**



**Fig 4.22: Variation of Total normal stress along the distance ( horizontal).**

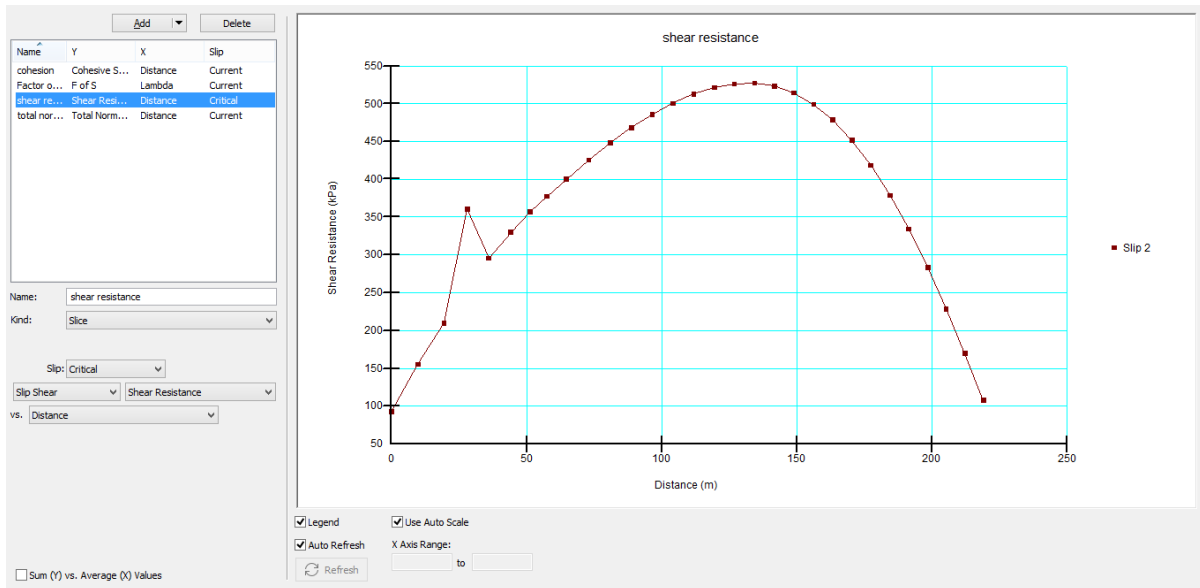


**Fig 4.23: Variation of shear resistance along the distance( horizontal).**

Vertical distance of 250m and horizontal distance of 500m has been considered here, rock layers considered are that of siltstone, but having varying rock parameters that is different GSI.

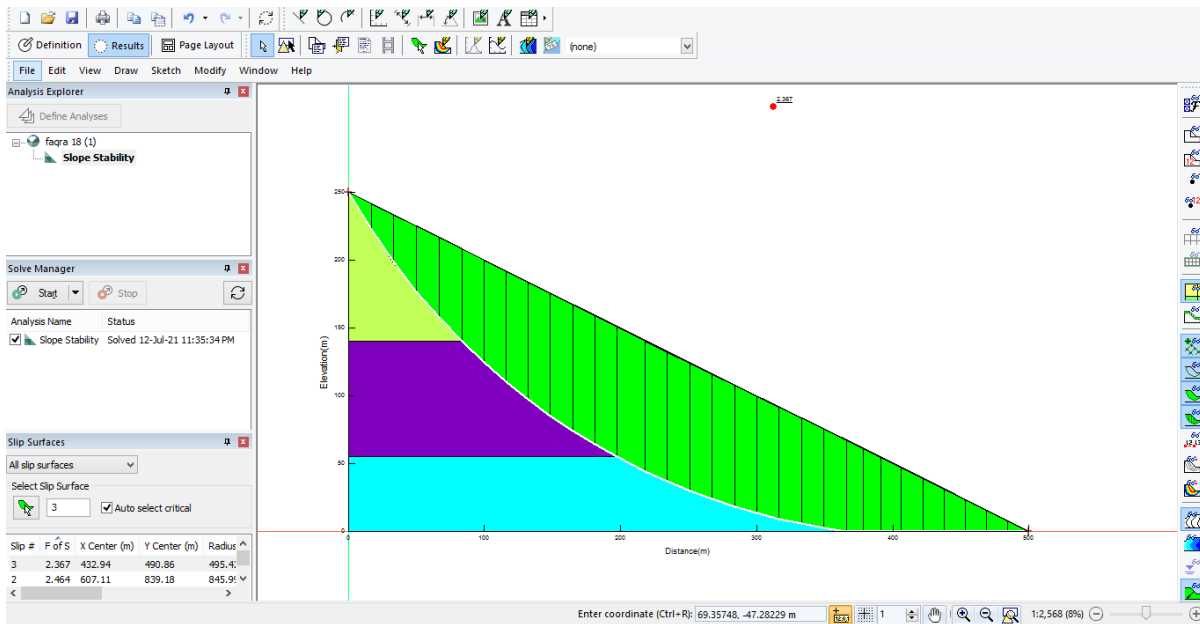


**Fig 4.24: F.O.S calculation and slip surface generation for 250m depth and 500m length.**

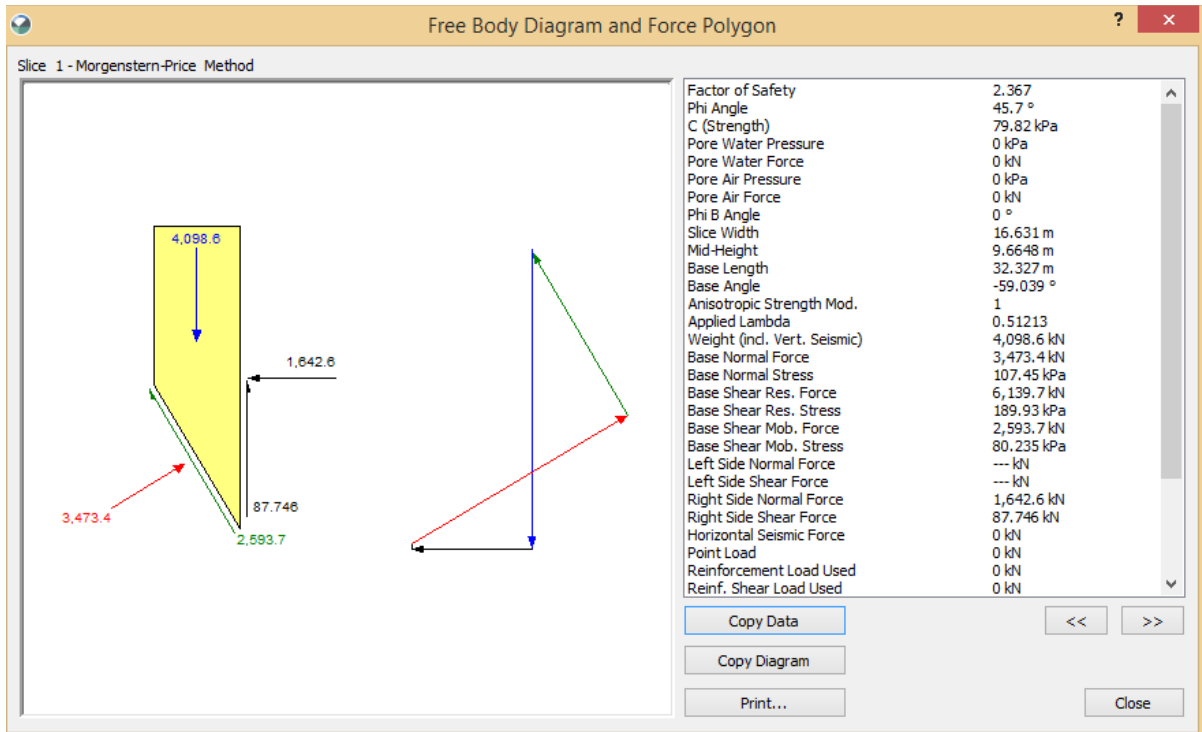


Fig 4.25: Body diagram for the forces acting on the slope.

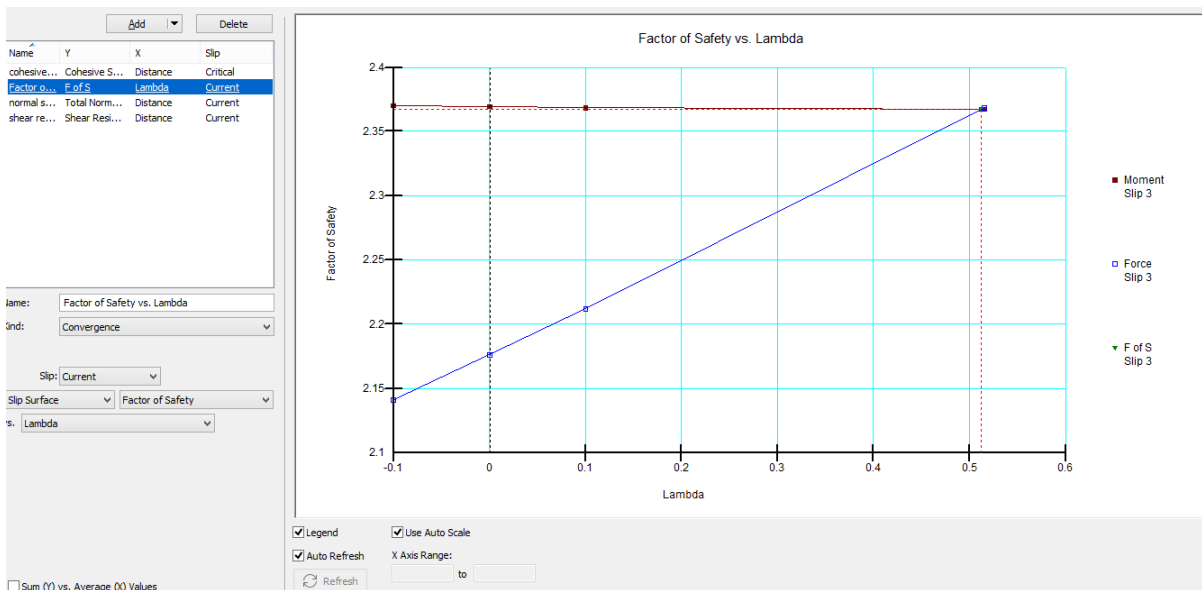
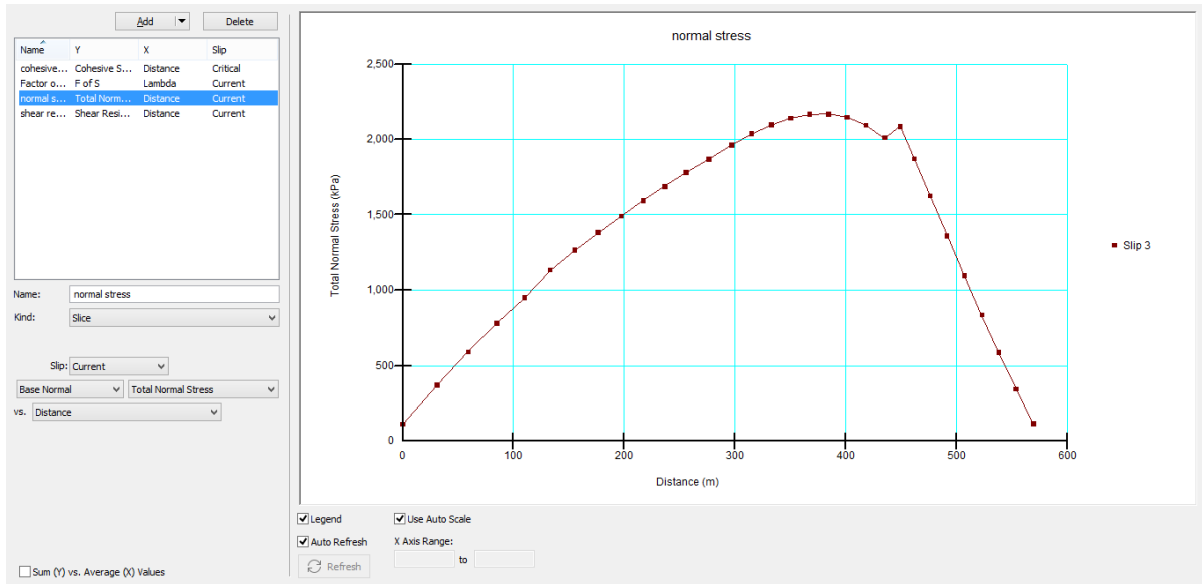
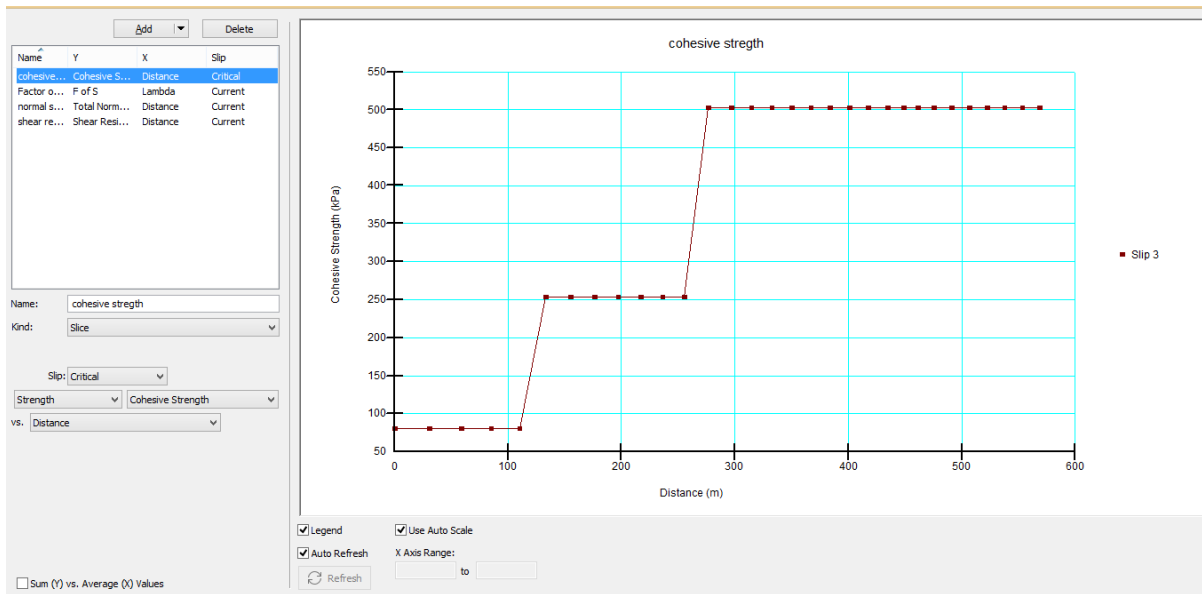


Fig4.26: F.O.S vs Lambda.



**Fig 4.27: Variation of Total normal stress along the distance ( horizontal).**



**Fig 4.28: Variation of cohesion along the distance( horizontal).**



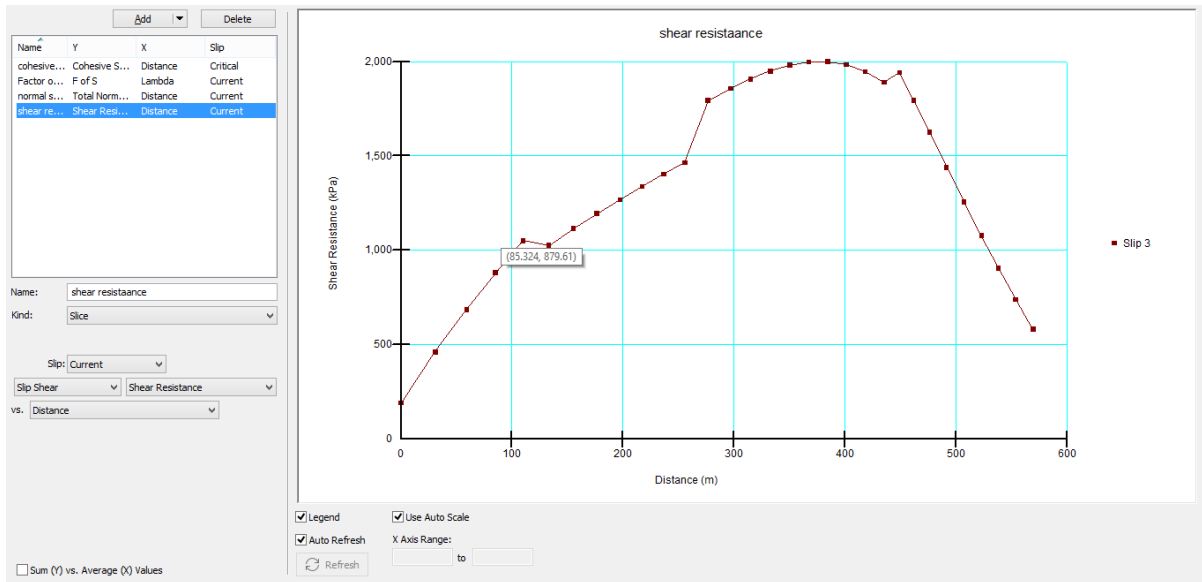


**Fig 4.29: Variation of shear resistance along the distance( horizontal).**

The ratio of vertical is to horizontal that has been considered is 1:3.

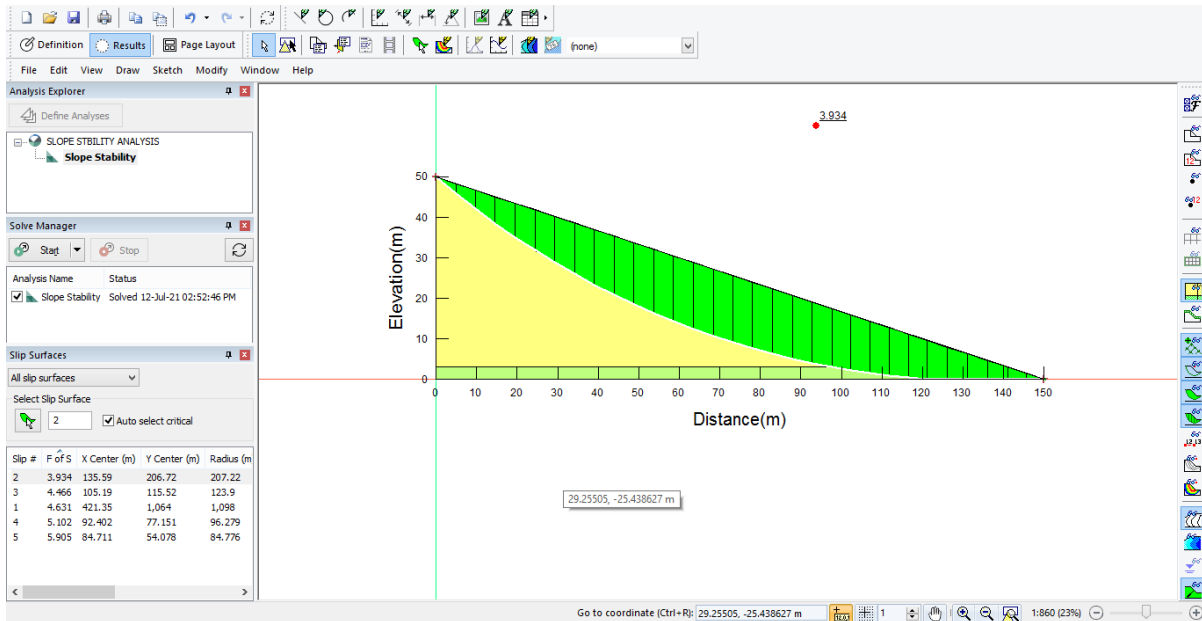


**Fig 4.30: F.O.S calculation and slip surface generation for 50m depth and 150m length.**

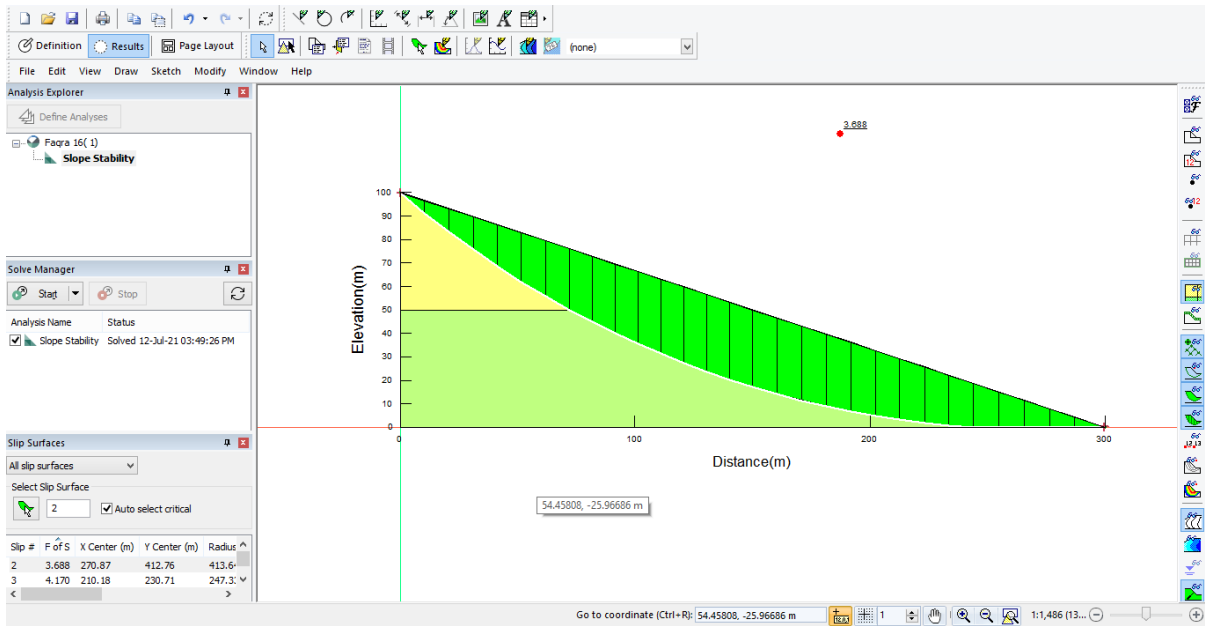


**Fig 4.31: F.O.S calculation and slip surface generation for 100m depth and 300m length.**

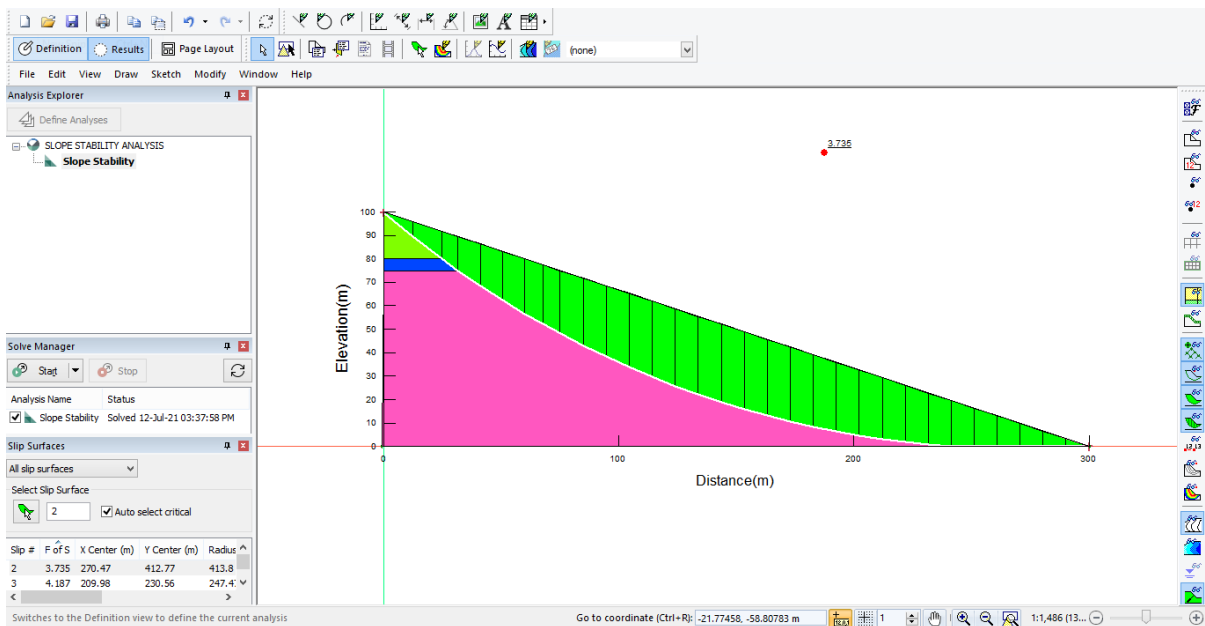


**Fig 4.32: F.O.S calculation and slip surface generation for 100m depth and 300m length.**

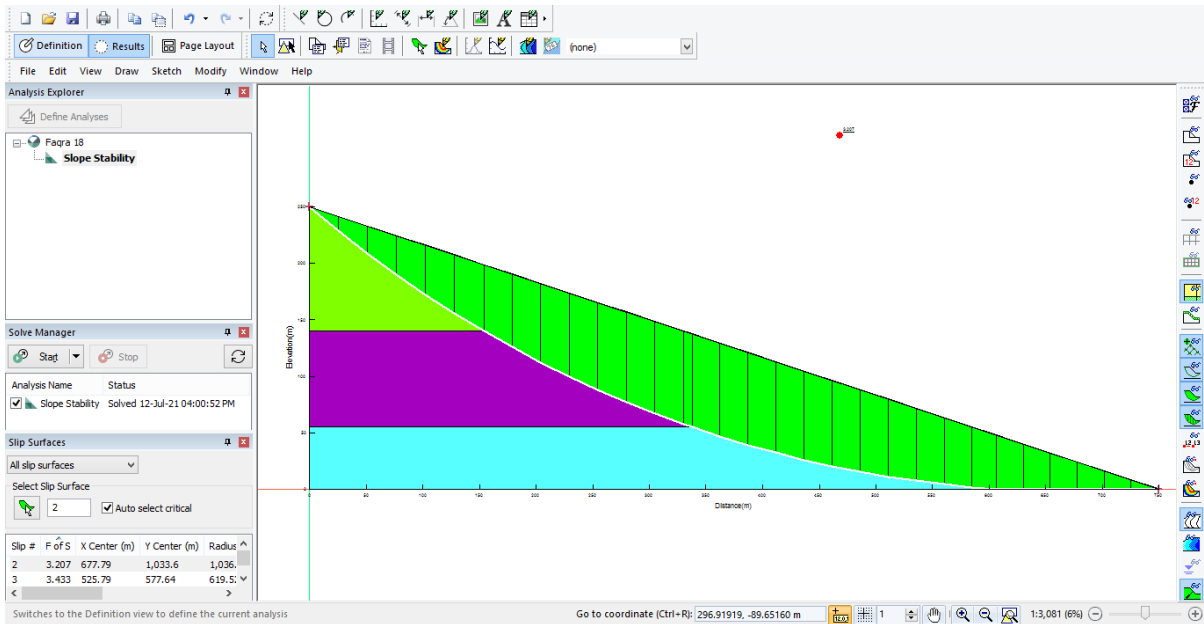


**Fig 4.33: F.O.S calculation and slip surface generation for 250m depth and 750m length.**

F.O.S of the slope has been calculated using two ratios 1:2 and 1:3. The F.O.S decreases with the increase of slope gradient. Also different F.O.S have been obtained based on the number of layers taken into consideration and the types of rock layers taken into consideration.

F.O.S vs  $\lambda(\Lambda)$  graph is the most important plot in the slope stability study. It includes both moment and force factors of safety. The converge factor of safety for each slip surface is found at the intersection of moment and force F.O.S. Other graphs that have been obtained using the software are the variation of cohesion along the length. Similarly the variation of normal stress along the length of the slope and change in the shear resistance along the length have also been calculated and included in the report.

Force information of the critical slice is given by the body diagrams, which provide the horizontal and vertical forces acting on the slice. Multiple slip surfaces have also been shown in one slope, but mostly the critical slip surface has been shown. Failure

zone has also been shown in one of the models, safety map indicates the zone with slip surfaces having very similar factors of safety that have been developed.

The graphs that have been plotted that is normal stress vs the interslice distance, shear stress vs the interslice distance have almost a similar pattern that is increase then a peak and then decrease. This is because first the force acting of the slices goes on increasing and then at a critical slice F.O.S is calculated which becomes a peak and then there is a decrease in the after the peak in the consequent slides.

## **CHAPTER 5**

### **CONCLUSIONS AND RECOMMENDATIONS FOR FUTURE WORK:**

It is always necessary to model the underlying rock layer while evaluating stability of a slope having a rock layer overlain by a thick soil cover. The shear strength parameters of the soil are generally obtained from the laboratory tests while obtaining the same for rock-mass is a difficult task. So to overcome this problem, in the present study shear strength parameters (cohesion and angle of friction) of the weathered rock-mass were estimated using the method proposed by Hoek et al (2002). These estimated values were used to compute the factor of safety to obtain the stability state of the slopes. The study has shown the importance of field characterization of rock-mass for slope stability evaluation. The results obtained from the analysis were found to be in good agreement with the present field conditions. The strength envelope that is obtained from the Hoek Brown analysis is not a straight line, it is a curved line. It is observed that at the high stress level, the envelope curves down meaning it gives a low strength estimate than the Mohr Coulomb envelope. Factor of safety obtained after analysis is in the range of 1.07 to 2.25 implying that the slope is stable. The dynamic slope stability analysis has been obtained using Pseudo slope stability method and various graphs has been calculated. The dynamic shear strength of rocks at the site have not been calculated, once it is calculated Dynamic F.O.S can be calculated, this will give a better idea of slope stability at site. This is the future scope of the work that has been done. After this dynamic slope stability can also be simulated using QUAKE/W feature of the GEOSTUDIO software where with the use of acceleration Vs time graph of a particular magnitude earthquake can be used to perform the dynamic analysis.

## REFERENCES

1. Hoek, E. and Brown, E.T. 1980. Empirical strength criterion for rock masses. *J. Geotech. Engng Div., ASCE* 106 (GT9), 1013-1035.
2. Hoek, E. and Brown, E.T. 1980. *Underground Excavations in Rock*, London, Instn Min. Metall.
3. Hoek, E. 1968. Brittle failure of rock. In *Rock Mechanics in Engineering Practice* . (eds K.G. Stagg and O.C. Zienkiewicz), 99-124. London: Wiley
4. Brown, E.T. 1970. Strength of models of rock with intermittent joints. *J. Soil Mech. Foundn Div., ASCE* 96, SM6, 1935-1949.
5. Bieniawski Z.T. 1976. Rock mass classification in rock engineering. In *Exploration for Rock Engineering, Proc. of the Symp.*, (ed. Z.T. Bieniawski) 1, 97-106. Cape Town, Balkema.
6. Hoek, E. and Brown, E.T. 1988. The Hoek-Brown failure criterion - a 1988 update. *Proc. 15th Canadian Rock Mech. Symp.* (ed. J.C. Curran), 31-38. Toronto, Dept. Civil Engineering, University of Toronto.
7. Hoek, E., Wood D. and Shah S. 1992. A modified HoekBrown criterion for jointed rock masses. *Proc. Rock Characterization, Symp. Int. Soc. Rock Mech.: Eurock '92*, (ed. J.A. Hudson), 209-214. London, Brit. Geotech. Soc.
8. Hoek, E. 1983. Strength of jointed rock masses, 23rd. Rankine Lecture. *Géotechnique* 33 (3), 187-223.
9. Ucar, R. (1986) Determination of shear failure envelope in rock masses. *J. Geotech. Engg. Div. ASCE*. 112, (3), 303-315.
10. Londe, P. 1988. Discussion on the determination of the shear stress failure in rock masses. *ASCE J Geotech Eng Div*, 14, (3), 374-6.
11. Carranza-Torres, C., and Fairhurst, C. 1999. General formulation of the elasto-plastic response of openings in rock using the Hoek-Brown failure criterion. *Int. J. Rock Mech. Min. Sci.*, 36 (6), 777-809.
12. Hoek, E. 1990. Estimating Mohr-Coulomb friction and cohesion values from the Hoek-Brown failure criterion. *Intl. J. Rock Mech. & Mining Sci. & Geomechanics Abstracts*. 12 (3), 227-229.

13. Hoek, E. 1994. Strength of rock and rock masses, *ISRM News Journal*, 2 (2), 4-16.
14. Hoek, E. and Brown, E.T. 1997. Practical estimates of rock mass strength. *Intl. J. Rock Mech. & Mining Sci. & Geomechanics Abstracts*. 34 (8), 1165-1186.
15. Hoek, E., Kaiser P.K. and Bawden W.F. 1995. Support of underground excavations in hard rock. Rotterdam, Balkema.
16. Hoek, E., Marinos, P. and Benissi, M. 1998. Applicability of the Geological Strength Index (GSI) classification for very weak and sheared rock masses. The case of the Athens Schist Formation. *Bull. Engg. Geol. Env.* 57(2), 151-16